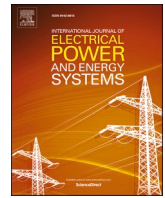


Contents lists available at [ScienceDirect](https://www.sciencedirect.com)

## International Journal of Electrical Power and Energy Systems

journal homepage: [www.elsevier.com/locate/ijepes](http://www.elsevier.com/locate/ijepes)

# Multi-stage and resilience-based distribution network expansion planning against hurricanes based on vulnerability and resiliency metrics

Amirhossein Nasri, Amir Abdollahi<sup>\*</sup>, Masoud Rashidinejad

Department of Electrical Engineering, Shahid Bahonar University of Kerman, Kerman, Iran

## ARTICLE INFO

### Keywords:

Distribution network expansion planning  
Resiliency  
Hurricane  
Automation  
Resilience indexes

## ABSTRACT

Distribution networks should be expanded to supply reliable and cost-effective services for new and existing customers to respond to the rising demand. On the other hand, there is an increasing awareness of resilience in the face of high impact low probability events. Therefore, this paper presents a multistage, dynamic, and resilient distribution network expansion planning framework to expand a distribution network resiliently. The proposed model is constructed as a six-step structure. The first step develops a network expansion topology. The hurricane occurrence model is executed in the second one that introduces a novel vulnerability index to recognize the most vulnerable facilities. Resilient planning based on the resilience resources such as distributed generations, hardening actions, and distributed automation systems is performed as the third step to reinforce the network preventive capabilities. In the fourth step, a resilient operation is considered to decrease unserved loads and restore the distribution system rapidly. Resiliency evaluation based on technical, financial, and social welfare metrics is employed as the fifth step. Finally, the non-dominated sorting genetic algorithm II optimization method operators are implemented in the sixth step to optimize the problem. Numerical simulations are performed on a 20 nodes distribution system and a real network. The results demonstrate the effectiveness of the proposed method.

## 1. Introduction

Due to the load increment, electric power distribution networks should be expanded to supply resilient and cost-effective services to added and existing consumers. Planners take into account the existing grid, load and price anticipation, technical and financial factors to estimate the optimal size, place, and time in which a substation or a line must be employed [1]. The proposed expansion topology should be coordinated with the strategic plans of companies that are usually employing a smart system with technologies such as advanced metering, energy storage system (ESS), automation, distributed generation (DG), and demand response [2]. In this way, reference [3] suggests a convex framework for distribution network expansion planning (DNEP) in presence of ESSs. Moreover, different active management strategies such as DG curtailment, on-load tap adjustment, demand response program, and reactive power compensation are employed in [3]. Reference [4] considers a two-level structure that is capable to give the probability that no technical limitations will present as a function of the reinforcement cost with and without employing DR and/or reconfiguration. In [5], a novel model based on the Z-number definition is employed to

take into account the presence of electric vehicle uncertainty and evaluate their effects on DNEP. Authors in [6] present a dynamic investment decision-making challenge arising in a distribution network within a transactive energy environment. Moreover, the main part of studies done in the context of DNEP tries to suggest approaches to consider the nonlinear and discrete situation of the mentioned problem and introduce effective optimization methods [7]. Most of the DNEP techniques presented in the literature optimize a cost-based objective function [7]. The operation cost and the investment cost are the main terms of this optimization function [8]. In [9], the maintenance cost is also considered. In the context of DNEP, the preventive studies against high impact low probability (HILP) events in the expansion planning procedures of distribution systems have not been discussed. On the other hand, recently, HILP disasters have progressively affected electric distribution networks over the world. As a result of climate change, natural phenomena can be happened usually and with higher intensity in the future [10]. The global concentration on unfavorable effects of HILP events on electric distribution systems has resulted in an increasing need to illustrate the resiliency of power systems. Resilience is the capability of a system to predict HILP events, stand against them, tackle their resilience-oriented preventive scheduling of microgrids (MGs) against

<sup>\*</sup> Corresponding author.

E-mail address: [a.abdollahi@uk.ac.ir](mailto:a.abdollahi@uk.ac.ir) (A. Abdollahi).

<https://doi.org/10.1016/j.ijepes.2021.107640>

Received 28 November 2020; Received in revised form 12 August 2021; Accepted 18 September 2021

Available online 8 October 2021

0142-0615/© 2021 Elsevier Ltd. All rights reserved.

Nomenclature	
<b>Indices and Sets</b>	
$N_{type}^L$	Number of line types
$\Omega^{sb}/N^{sb}$	Set/number of the existing and proposed substations
$N_{type}^{sb}$	Number of substation types
$\Omega^L/N^L$	Set/number of the existing and proposed lines
$\Omega^B/N^B$	Set/number of the load buses
$\Omega^{NHA}/N^{NHA}$	Set/number of buses not supported by hardening and automation
$N_j^C/N_j^{S-C}$	Number of total/supplied customers of bus $j$
$N_j^C/N_j^{D-C}$	Supplied customer number of bus $j$ in normal/disaster situation
$\Omega^{T-L}/N^{T-L}$	Set/number of tie-lines
<b>Parameters and Constants</b>	
$C_{inv}/C_{opr}$	Total investment/operation cost of expansion topology (\$)
$C_{loss}$	Cost per unit of energy lost (\$/kWh)
$OC^{sb}$	Substation operation cost (\$)
$\delta_v$	Maximum allowable voltage variation (perunit)
$C^H$	Line hardening cost (\$/km)
$C^{Shed}$	Cost per unit of load shedding (\$/kW)
$T^R$	Time horizon of operation (Hour)
$t_a^{DG}$	DG synchronization time with type $a$
$\omega$	Hurricane speed (m/s)
$V_{norm}$	Nominal voltage of the network (kV)
$\gamma_n$	Priority of bus $n$
$t_{start}$	HILP event occurrence time (Hour)
$t_a^{SW}$	Switch delay time with type $a$ (Hour)
$t_{AS}^{SW}$	Automatic switch delay time (Hour)
$ERI^{Cons}$	ERI index maximization constant (\$)
$ERI^{Base}$	ERI index base (\$)
$\eta_m$	Mutation index
$\rho^C$	Crossover probability
$\hat{E}^{DEC}$	DECcoefficient
<b>Function and variables</b>	
$V_j(t)$	Voltage of bus $j$ at year $t$ (kV)
$DGPIn$	DG priority index of bus $n$
$F_{DNEP}$	DNEP objective function (\$)
$LSC$	Total load shedding cost (\$)
$DEC$	Damaged equipment cost (\$)
$RIC$	Resiliency investment cost (\$)
$HC$	Total hardening cost (\$)
$DGC$	Total DG investment cost (\$)
$ASC$	Total automation system cost (\$)
$Q_j^L$	Reactive power flow in line $j$ (kVA)
$Q_j^{sb}$	Reactive power supplied by substation $j$ (kVA)
$cd_j$	Crowding distance of solution $j$
$P_j^{sb}$	Active power supplied by substation $j$ (MW)
$B^D$	Line vulnerability threshold
$P_j^{L, Loss}$	Active power loss of line $j$ (MW)
$P_j^{B, Min}$	Minimum supplied power of bus $j$ (MW)
$P_n^B$	Active power of load bus $n$ (MW)
$P_j^L$	Active power flow in line $j$ (MW)
$F_i^{max}/F_i^{min}$	Maximum/minimum of the $i$ th objective function
$\Omega^{V-L}$	Set of the most vulnerable lines
$t, T$	Index and number of time horizon of planning
$\Omega_j^{D-L}$	Set of the downstream buses of line $j$
$N_{type}^{DG}$	Number of DG types
$t^{Opt}, T^{Opt}$	Index and the number of NSGA-II iterations
$N^F$	Number of objective functions
$N_f^L/N_f^B$	Line/bus number of a feeder
$\Omega^S/NS^{Opt}$	Set/ number of the NSGA-II solutions
$x^{Cnt}$	Feeder connection status
$IC_a^L$	Line investment cost with type $a$ (\$/km)
$IC_a^{sb}$	Investment cost for a substation of type $a$ (\$)
$IC_a^{DG}$	DG investment cost of type $a$ (\$)
$IC_{AS}^{SW}$	Automatic switch investment cost (\$)
$\theta^j/\theta^H$	Line/hurricane angle differences to the north-south direction ( $^\circ$ )
$R$	Annual interest rate of investment
$B_P^D/B_O^D$	Line vulnerability threshold in pre-step of resilient planning/ operation
$S_j^{sb, max}$	Capacity of substation $j$ (MVA)
$S_j^{L, max}$	Capacity of line $j$ (MVA)
$L_j$	Length of line $j$ (km)
$RB$	Resilience budget (\$)
$V_j^R$	Rated voltage of bus $j$ (kV)
$t_{MS}^{SW}$	Manual Switch delay time (Hour)
$P^{TB}$	System total load (MW)
$TRI^{Base}$	TRI index base
$\eta_c$	Crossover index
$\rho^m$	Mutation probability
$IC_{MS}^{SW}$	Manual switch investment cost (\$)
$ERI$	Economical resiliency index
$ASIJ$	Automatic switch priority index for tie-line $j$
$SWRI$	Social welfare resiliency index
$TRI$	Technical resiliency index
$SRI$	System robustness index
$PAI$	Power adaptability index
$NRI$	Network recovery index
$VI_j$	Vulnerable index of line $j$
$P_j^{B, Shed}$	Load shedding of bus $j$ (MW)
$\omega^{max}$	Maximum predicted hurricane speed (m/s)
$F_i$	The $i$ th objective function
$x_{j,t,a}^{sb}$	Status of substation $j$ at year $t$ with type $a$
$x_{j,t,a}^{Sw}$	Status of switch $j$ at year $t$ with type $a$
$x_{j,t,a}^L$	Status of line $j$ at year $t$ with type $a$
$x_{j,t,a}^{T-L}$	Status of ti-line $j$ at year $t$ with type $a$
$x_{j,t,a}^{L-H}$	Hardening status of line $j$ at year $t$ with type $a$
$x_{j,t,a}^{DG}$	Status of DG $j$ at year $t$ with type $a$
$x_{pf}^{Cnv}$	Power flow convergence status
$P_j^{B,R}$	Rated power of load bus $j$ (MW)

the impacts of HILP disasters in a proactive technique, and fast restore from the degraded condition [11]. Furthermore, resilience goes beyond the consequences on customers and concentrates on how fast and efficiently the facilities is recovered to its pre-disaster operational situation

[11]. Resilience-improvement actions have been classified into hardening-oriented, planning-oriented, and operation-oriented actions [11]. Hardening-oriented actions are applied to reinforce the components and reduce the vulnerability of infrastructures in extreme events. Elevating

substations, strengthening poles and facilities with stronger materials, and vegetation management can be mentioned as hardening-oriented actions against HILP events [11]. In the field of hardening-oriented actions in resilience improvement of electric systems, an explanation of the pivotal notions of power systems resilience is provided in [11] to apply the hardening and smart operational techniques to enhance it. In [12], a hardening strategy framework of overhead lines for the diminution of the damage is proposed that is caused by typhoons to distribution networks in typhoon-prone regions. The suggested structure considers typhoon motion directions and computes the line load reliability under extreme weather. A robust optimal line hardening approach coupled with multiple provisional MGs is proposed in [13] to enhance the resiliency of a distribution network against worst N-k contingencies. A deterministic single crew approximation model with two solution approaches, mixed-integer linear programming (MILP) formulation and a heuristic method are suggested in [14] to harden distribution networks against natural phenomena. Reference [15] introduces a deterministic hardening planning framework to reduce the long-term network risk of load curtailment, which reduce the computational cost concern. Due to accomplish the mentioned task, a set of events with corresponding load curtailments and load loss are achieved by an enhanced Monte Carlo method. A tri-level robust optimization-based approach for system hardening is employed in [16] to minimize the worst-case total weighted electricity and gas load curtailment of integrated electricity and natural gas distribution systems with respect to hardening budget constraints and random failures happened by phenomena of several severity levels. Reference [17] studies the system lines hardening in the field of stochastic power flows injected by the high penetration of renewable energy. In [18], due to enhancing the resilience of the system, repairing, and upgrading of system poles and vegetation management are used as the system hardening solutions. Planning-oriented actions consider employment size, type, and place of DGs, ESSs, parking lots, and automation devices to enhance the preventive and recovery capabilities of systems against different HILP events. In this field, reference [19] proposes an innovative planning technique for the resilience improvement of an electric grid, including specifying the sectionalizing-based optimal black start resources placement of ESSs during HILP disasters. Authors in [20] present a multi-year and multi-criteria generation planning to resiliently provide power by renewable energy resources. In [21], a novel resilience metric based on social welfare notion is suggested to reduce unserved loads, recover the electric distribution network fast and reduce the reliance of water network operation on distribution system damages. The novel resilience metrics are optimized with effective techniques including upgrading distribution poles, DGs allocation, and automation infrastructures. The planning of microgrids is suggested in [22] to strengthen the system against extreme faults. In this way, several methods are introduced to recognize the optimal buses for the connection of microgrids and the capacity of the dispatchable resources used within microgrids. Operation-oriented actions refer to preventive and control-based approaches applied to make a distribution network capable of dealing with the effects of an HILP event when it happens [11]. With the appearance of advanced visualization and smart technologies, real-time state awareness of distribution networks is becoming viable. The operation-oriented actions can be effectively implemented using real-time monitoring data so that the distribution network resilience is protected in the HILP phenomena situation. Conservation voltage regulation, defensive islanding, generation reschedule and priority-based load curtailment can be mentioned as operation-oriented actions implemented when an HILP disaster unfolds. In opposition to hardening-oriented and planning-oriented actions which are passive, costly, and long-term strategies to reinforce the distribution network, operation-oriented actions are proactive, real-time, and low-cost remedies to promote the system resiliency capability. In the field of operation-oriented actions in resilience enhancement of power systems, reference [23] suggests stochastic indexes to evaluate the operational resilience of the power systems to HILP phenomena. An

innovative risk-based defensive islanding is suggested in [24] which reduces the cascading disaster during extreme weather conditions. The fuzzy-Markov model is suggested in [25] for modelling and considering the effects of lightning uncertainty on the performance of a supplier in a smart grid in the presence of renewable energies, demand response programs, and energy storage systems. Authors in [26] optimize the framework of ESSs on electrical power networks for resilience to failure happened by HILP phenomena under a high penetration scenario for rooftop photovoltaic units. Reference [27] presents the role of operation-oriented proactive actions in improving power grid resilience. An explanation was also given on techniques and requirements of three levels of HILP disasters such as before, during, and after the disaster, to provide resilience against HILP disasters. In [28], an integrated structure to convert weather prediction into proper information is presented for preventive scheduling during hurricanes so that the interruptions induced by hurricanes can be decreased. An integrated preventive-corrective structure is proposed in [29] to enhance the power grid resilience against HILP events. The suggested framework implement situational awareness to improve resilience capability and ensures efficient strategies in both emergency and preventive operation conditions. In [11], operation-oriented actions for resilience enhancement are discussed. A comparison is also presented to distinguish operational and hardening actions. Reference [30] explains such main paths and novel progressions in energy delivery facilities resilience and operational resistance against cyber-attacks. A novel MG operation framework and resiliency considerations are suggested under the risk of load, prevailing uncertainties of renewable suppliers, and utility damage in [31]. Authors in [32] have used MG infrastructures to improve the MG resilience with a two-level probabilistic programming technique. In [33], a normal operation of MG is preventively promoted before the estimated disaster (i.e. disconnection from the upstream network) to provide feasible islanding at the disaster onset. In [34], a resilient operation model based on two operation modes (i.e. islanded and grid-connected) and technical detail, such as voltage-related operation limitations, is proposed for the resilience improvement of a hybrid AC/DC MG. An MG preventive management structure is suggested in [35] to cope with the adverse effects of extreme hurricanes. In [36] a recognition and reduction framework for cyber-attacks and sensor faults is proposed in a direct current MG to satisfy resilient operation in cyber-attacks and fault conditions. However, these previous studies do not consider how to expand and reinforce a distribution system simultaneously to improve the resiliency of a system against HILP events. Therefore, due to expand a primary distribution network in a way that its resiliency is improved against the HILP events, this paper presents a novel, multi-stage, dynamic, and resilience-based distribution network expansion planning structure that is constructed from six steps. The proposed model is named (RDNEP) against natural disasters by implementing innovative models for resiliency evaluation, planning and operation that is performed from a distribution company perspective. In the first step of the proposed framework, DNEP is performed to connect new loads to a distribution network based on investment and operation costs by determining the optimum paths and locations for new lines and substations, respectively. In the second one, a hurricane is considered as a natural phenomenon in the present study. Associated with an upcoming hurricane, its geographical trajectory and metrological specifications are considered with the fragility curves of distribution lines, and those suspected to go out of service are recognized through a novel model that considers the lines importance, the hurricane speed and direction as well as the line fragility curve simultaneously as a novel vulnerability index (VI). Then, the suggested framework searches the reinforcement and modification strategies for the expanded distribution network according to the novel proposed structure and indexes which improves the resiliency of a distribution network based on DGs placement, line hardening actions, and distribution system automation as the third step. In the fourth step, the vulnerability of the expanded and reinforced network is determined against the phenomenon by executing the phenomenon

**Table 1**  
Taxonomy of the reviewed papers.

References	Resilient operation	Resilient planning	DNEP	Hardening	HILP event	Resilience index
[8]	–	–	✓	–	–	–
[11]	✓	–	–	✓	Windstorms	A set of resilience metrics
[17]	–	–	–	✓	Extreme weather events	Load shedding
[19]	✓	✓	–	–	Extreme weather events	Load shedding
[20]	–	✓	–	–	Extreme weather events	Load shedding
[21]	✓	✓	–	✓	Hurricane	Technical & social welfare metrics
[23]	✓	–	–	–	Extreme weather events	Probabilistic metrics
[24]	✓	–	–	–	Windstorms	Load shedding
[26]	✓	–	–	–	Extreme weather events	Load shedding
[30]	✓	–	–	–	Cyber attacks	Load shedding
Present paper	✓	✓	✓	✓	Hurricane	Technical, financial & social welfare indexes

occurrence model. Then, proactive scheduling is employed to minimize the effects of lines outage, and load curtailment at the event onset. In this step, the operation-oriented preventive actions including network reconfiguration and generation reschedule are accommodated which keep the low vulnerable branches in the service while satisfying the most load. After that, the resiliency of the expanded and reinforced topology is evaluated by the proposed technical, financial, and social welfare (TFS) metrics based on the outcomes of the above-mentioned steps. In the proposed framework, the discussed problem is modeled as a mixed-integer nonlinear programming (MINLP) problem. Due to the complex nature of this problem, the non-dominated sorting genetic algorithm II (NSGA-II) and the technique for order preference by similarity to ideal solution (TOPSIS) approach is employed to optimize the expansion and reinforcement structure of a distribution network based on an iterative manner. The innovative contributions of this study considering the attributes of the works analyzed in the literature review which has been depicted in Table 1, summarized as follows:

- A multi-stage and dynamic framework is presented to resiliently expand and reinforce a distribution network.
- Due to evaluate the vulnerability of a network against a hurricane, an innovative model is proposed by considering a novel vulnerability index based on the line fragility curve, line importance, and line deference angle from the hurricane path.
- A set of technical, economic, and social welfare indexes are proposed as TFS metrics to evaluate different resiliency aspects of a distribution network system.
- In order to determine the line hardening topology properly as well as the locations of DGs, and automation devices, a set of novel planning indexes and an innovative method are proposed.
- An iterative optimization method is proposed based on a common and proper multi-objective algorithm by considering DNEP, resilient planning and scheduling, hurricane occurrence model, and resiliency evaluation at each iteration.

The rest of this study is constructed as follows: Section two presents the problem definition. Section three discusses how the problem is executed by the proposed framework. Numerical results are presented in section four and section five concludes the paper.

**Table 2**  
Detail of the problem variables.

Variable	Value	Definition
$x_{j,t,a}^L$	+1	Added line $j$ with type $a$ at year $t$ .
	0	Not changed line $j$ with type $a$ at year $t$ .
	–1	Removed line $j$ with type $a$ at year $t$ .
$x_{j,t,a}^{H-L}$	+1	Hardened line $j$ with type $a$ at year $t$ .
	0	Not hardened line $j$ with type $a$ at year $t$ .
$x_{j,t,a}^{T-L}$	+1	Added tie- line $j$ with type $a$ at year $t$ .
	0	Not added tie-line $j$ with type $a$ at year $t$ .
$x_{j,t,a}^{Sb}$	+1	Added substation $j$ with type $a$ at year $t$ .
	0	Not added substation $j$ with type $a$ at year $t$ .
$x_{j,t,a}^{DG}$	+1	Added DG $j$ with type $a$ at year $t$ .
	0	Not added DG $j$ with type $a$ at year $t$ .
$x_{j,t,a}^{SW}$	+1	Added switch $j$ with type $a$ at year $t$ .
	0	Not added switch $j$ with type $a$ at year $t$ .

**2. Problem definition**

Due to urbanization and industrial development, a considerable rise in energy demand has happened in recent years. To satisfy the load increase optimally and consider the pseudo-dynamic manner of several grid parameters, the DNEP is required. Distribution network capacity expansion contains reinforcement and installation of substations, feeders, and DGs. On the other hand, due to climate alteration, the number and intensity of disasters against essential facilities have been increased during recent years. Hurricanes, floods, and earthquakes as HILP events cause considerable failures of critical facilities and life-sustaining goods cannot be achieved. HILP events may affect greatly the resiliency of distribution network operation. Climate change studies illustrate that the number and intensity of HILP disasters might grow soon [10]. Therefore, distribution networks require to be not only reliable to the common events but also be resilient to HILP phenomena. In this way, the main problem of this study is determining a distribution network expansion topology that is capable in front of HILP events as the proposed RDNEP framework. Therefore, the main decision variables that should be determined in this problem are organized as Fig. 1. These variables are classified as, expansion lines, tie-lines, hardened lines, substations, DGs, and switches variables. These variables determine the location, type, and time of infrastructure installation. Moreover, Table 2 presents the detail of the above-mentioned variables.

...	Element $j$						...	
...	...	Year $t$			Year $t+1$			...
...	...	Type 1	Type 2	...	Type 1	Type 2	...	
...	...	$x_{j,t,1}$	$x_{j,t,2}$	...	$x_{j,t+1,1}$	$x_{j,t+1,2}$	...	

Fig. 1. Variables structure.

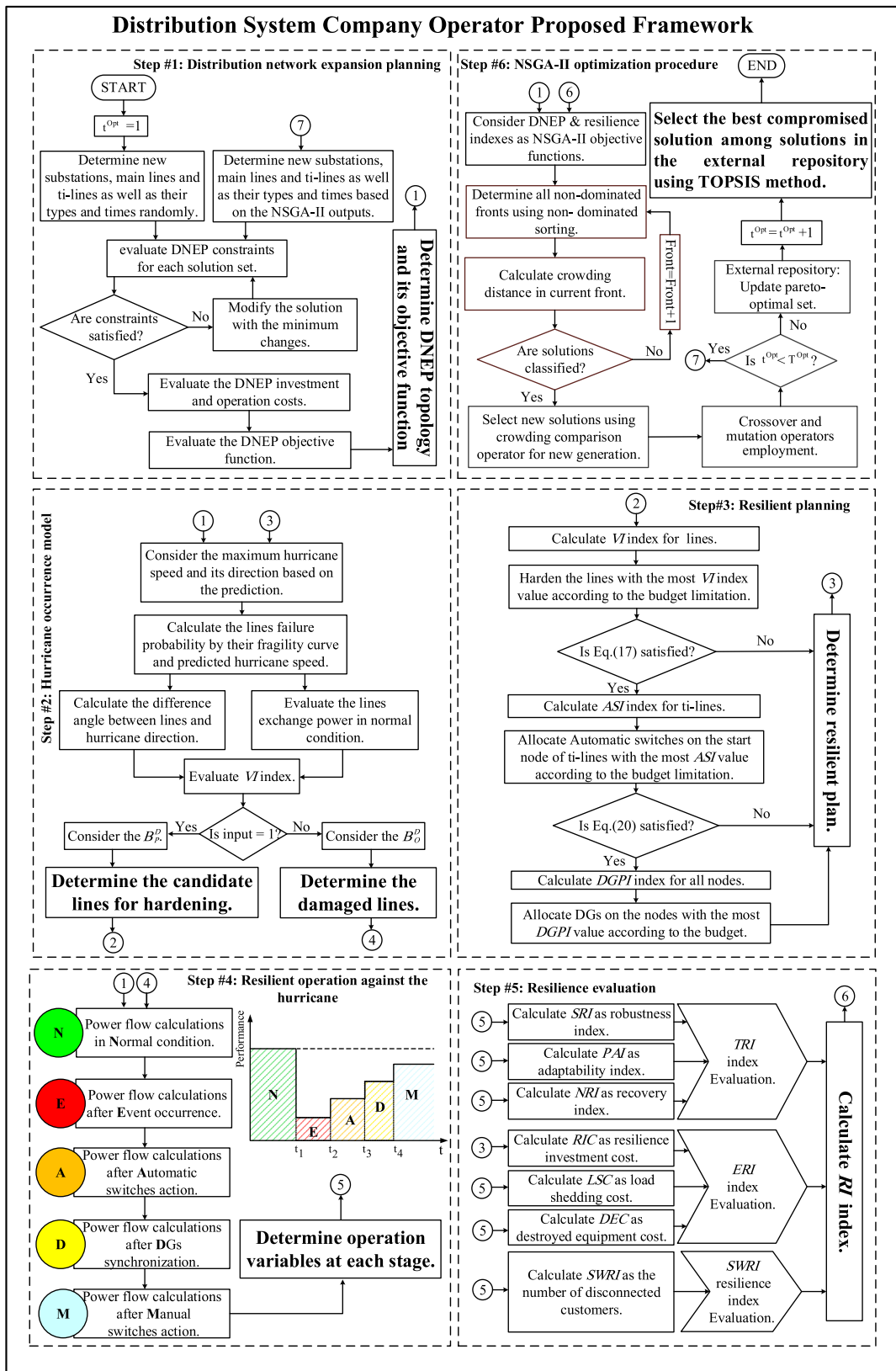


Fig. 2. The proposed RDNEP framework.

### 3. The proposed RDNEP framework

In order to preventively expand and reinforce a distribution network simultaneously against HILP events, this paper suggests a dynamic and

multi-stage structure as shown in Fig. 2. This structure is constructed from six steps. The RDNEP framework steps consist of DNEP, hurricane occurrence model, resilient planning, resilient operation, resilience evaluation, and NSGA-II optimization procedure. In the proposed

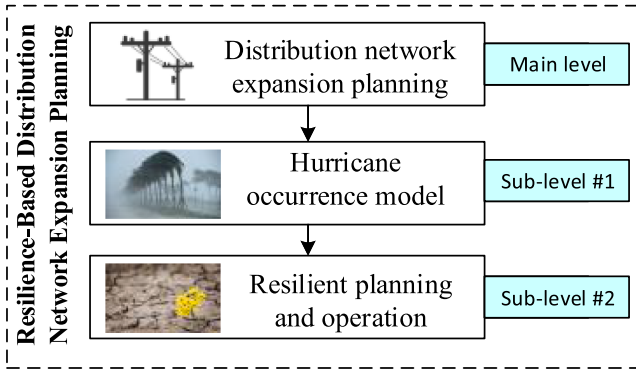


Fig. 3. The optimization structure of RDNEP.

framework, NSGA-II is considered as the main optimization method that its operators (i.e. crowding distance calculation, non-dominated sorting, crossover, mutation, and selection [37]) are executed on the solutions of each iteration in the sixth step of RDNEP. The other steps decide for the variables, limit the search space, check the constraints or evaluate the objective functions to prepare the requirements of the main optimization procedure that is executed in the sixth step of RDNEP. In this way, DNEP as the first step of the proposed framework determines the expansion planning variables (i.e. lines and substations) that are performed randomly in the first iteration and determined based on the outcomes of step #6 in the other iterations. Moreover, this step evaluates and satisfies the DNEP constraints, and calculates the DNEP cost as the first RDNEP objective function. Therefore, optimization is not performed at this step. However, the DNEP variables are prepared for the main optimization procedure at step #6. In the hurricane occurrence step, the vulnerability index against a hurricane is evaluated for the whole lines of each solution. Then, the lines will be sorted based on the VI metric and the lines that have the most VI value are considered as candidate lines for the hardening in the first time or the damaged lines in

divide the problem-solving procedure into several sections. It causes the number of variables that should be determined and optimized at each step reduced. More clarification for the mentioned steps are presented as follows:

On the other hand, the RDNEP optimization structure is presented in Fig. 3. RDNEP is created from a main optimization level and two sub-levels. The main level is constructed from the distribution network expansion model and NSGA-II procedure steps. Sub-level #1 consists of the hurricane occurrence model and sub-level #2 is made from resilient resources allocation, resilient operation, and resilience evaluation steps.

### 3.1. DNEP procedure

This step determines the DNEP variables such as location, type, and time of lines and substations according to the technical constraints to connect new loads to an existing distribution network as a distribution network expansion topology at each optimization algorithm iteration. In this way, if the iteration variable is equal to one (i.e.  $t^{Opt} = 1$ ), the initial solutions for expansion topology are specified randomly. Then, DNEP constraints are checked. If the whole DNEP constraints are satisfied, DNEP investment and operation costs are evaluated as Eqs. (1) and (2) [38], respectively. After that, DNEP objective function can be calculated by Eq. (3). If DNEP constraints are not satisfied, due to evaluate the DNEP costs and objective function, the solutions should be modified by the minimum changes to satisfy the whole DNEP constraints. In the other iterations (i.e.  $t \neq 1$ ), the output of the NSGA-II algorithm in the previous iteration is considered as input of this section that is shown in Fig. 2.

$$C_{Inv} = \sum_{j=1}^{N^{sb}} \sum_{t=1}^T \sum_{a=1}^{N^{type}} \frac{x_{j,t,a}^{sb}}{(1+r)^{t-1}} \times IC_a^{sb} + \sum_{j=1}^{N^L} \sum_{t=1}^T \sum_{a=1}^{N^{type}} \frac{x_{j,t,a}^L + x_{j,t,a}^{T-L}}{(1+r)^{t-1}} \times IC_a^L \quad (1)$$

$$C_{Opr} = \sum_{j=1}^{N^{sb}} \sum_{t=1}^T \sum_{a=1}^{N^{type}} \frac{x_{j,t,a}^{sb}}{(1+0.5r)^{2t+1}} \times (8760 \times S_j^{sb,max}(t) \times OC^{sb}) + \sum_{j=1}^{N^L} \sum_{t=1}^T \sum_{a=1}^{N^{type}} \frac{x_{j,t,a}^L + x_{j,t,a}^{T-L}}{(1+0.5r)^{2t+1}} \times (8760 \times P_j^{L,Loss}(t) \times C^{Loss}) \quad (2)$$

the second time of executing this step according to the vulnerability budget. In the resilient planning step, the variables for the resilient resources (i.e. hardened lines, automatic switches, and DGs locations) should be determined. In this step, instead of determining the mentioned variables randomly, they are defined based on the appropriate indexes and economic budget constraints that are explained in the following. In this step, the allocation indexes for resilience resources are calculated and sorted. Then, the locations that have the maximum values are determined as the resilience resources variable according to the budget constraint. In the resilient operation step, after determining the more probable damaged lines by the hurricane occurrence model, according to the location of isolated loads, resilience resources are employed. Then, power flow calculations are applied at each operating state to evaluate the required variables for the resiliency evaluation step. The resilient evaluation step is implemented to calculate the resilience index as the second objective function of RDNEP. In this step, optimization is not implemented. However, different resilience indexes are calculated based on the outcomes of the previous steps. Therefore the complexity of the problem is reduced in comparison with the one-step framework that the whole variables should be considered and optimized, simultaneously. These steps are performed sequentially. It means that the output of one step is employed as the input of the next step. These steps

$$F_{DNEP} = C_{Inv} + C_{Opr} \quad (3)$$

Both investment and operation costs consist of two terms based on feeder and substation costs. The technical DNEP constraints that should be satisfied are presented as follows:

$$x^{Cont} = 1 \quad (4)$$

$$N_f^L = N_f^B \quad (5)$$

$$x_{pf}^{Cnv} = 1 \quad (6)$$

$$P_j^{sb,2}(t) + Q_j^{sb,2}(t) \leq S_j^{sb,max,2}(t), \forall j \in \Omega^{sb} \& t \in \{1, 2, 3, \dots, T\}$$

$$P_j^{L,2}(t) + Q_j^{L,2}(t) \leq S_j^{L,max,2}(t), \forall j \in \Omega^L \& t \in \{1, 2, 3, \dots, T\} \quad (8)$$

$$(1 - \delta_V) V_{norm} \leq V_j(t) \leq (1 + \delta_V) V_{norm}, \forall j \in \Omega^B \& t \in \{1, 2, 3, \dots, T\} \quad (9)$$

$$0 \leq \sum_{t=1}^T \sum_{a=1}^{N^{type}} x_{j,t,a}^L + x_{j,t,a}^{T-L} \leq 1, \forall j \in \Omega^L \quad (10)$$

$$0 \leq \sum_{t=1}^T \sum_{a=1}^{N_{type}^{sb}} x_{j,t,a}^{sb} \leq 1, \forall j \in \Omega^{sb} \quad (11)$$

Eq. (4) is employed to determine that the whole buses are connected to the grid by a feeder and there is no isolated bus. To specify the amount of  $x^{Cnt}$ , the proposed grid topology is traversed to specify whether each feeder is a connected topology (i.e.  $x^{Cnt} = 1$ ) or not (i.e.  $x^{Cnt} = 0$ ). Since a grid is radial, each feeder is a connected topology, and the number of lines ( $N_l^r$ ) is as same as the number of buses ( $N_b^r$ ). Eq. (5) is an adequate situation for grid radiality without considering the tie-lines [7]. Eq. (6) evaluates the convergence of the power flow computations by using one of the power flow results based on a binary variable (i.e.  $x_{pf}^{Cnv}$ ).  $x_{pf}^{Cnv}$  equals one if computations converge and equals zero if power flow diverges due to mismatch of reactive or active power at each bus. Eqs. (7) and (8) depict the capacity of the lines and substations, sequentially. Eq. (9) illustrates the limitations of the voltage value of buses. The substation and line presence constraints are depicted as Eqs. (10) and (11), sequentially. On the other hand, due to connecting the new loads to the distribution network for several years and prevent capital blocking in the time horizon of planning, DNEP as the first step of RDNEP should be performed dynamically. In this way, the variables are defined time-based according to their employment time as depicted in Fig. 1 and constraints (10) and (11). These constraints ensure that in a path/location during the planning horizon, just one line/substation can be installed. Moreover, it should be noted that the planning problem is not

overhead lines will be determined by the lines fragility curve and predicted hurricane speed [41]. In the fragility curve, the damage level of hurricanes is modeled and considered as the failure probability based on the hurricane speed. In a distribution network, lines and poles have the most vulnerability against the hurricane and they are high consumption equipment. Therefore, the most existing references in this field such as [42] consider lines and poles vulnerability in the resiliency studies of distribution systems. According to reference [42], lines are more vulnerable than poles. Hence, this study considers lines fragility curve that satisfies the poles vulnerability. Moreover, lines difference angles from hurricane direction should be determined to evaluate the vulnerability of lines. After that, power flow calculations will be applied to evaluate the importance of the lines. Finally, the VI metric according to Eq. (12) is evaluated for all lines to determine the most vulnerable and curtail lines. It should be noted that at each algorithm iteration and each population member, the proposed expanded and resilient network topology as a problem solution will be changed and lines with different directions and various downstream loads will be employed. In this way, the hurricane occurrence model should be performed for each solution at each iteration separately to evaluate the lines' vulnerability. Therefore the independent optimization level for the hurricane occurrence model can not consider the changes of network for solutions and population members in different iterations. However, hurricane speed prediction is not dependent on the network topology. Therefore, it can be performed as an independent level and its result can be employed in the step of hurricane occurrence model [41].

$$VI_j = \left( \frac{|\Delta\theta_j - \Delta\theta_H|}{\Delta\theta_{90}} + \frac{\int_0^{\omega^{max}} f_j(\omega) \times d_\omega}{\int_0^{\omega^{max}} 1 \times d_\omega} + \frac{\sum_n \int \Omega_j^{D-L} \gamma_n \times P_n^B}{Max(\gamma \times P^B)} \right)$$

$$\forall j \in \Omega^L \quad (12)$$

real-time scheduling. Therefore, its time-consuming feature will not be a concern or challenge. Hence, the network designer has enough time to solve the problem. It should be noted that the variables of this step will be optimized by NSGA-II operators in step #6 after considering the result of other steps. To satisfy the above-mentioned constraints, the rejecting method is applied for dealing with the constraints (4), (5), (6), (10), and (11) in which the infeasible chromosomes are discarded all over the generations according to reference [39] and [2]. However, for violation of constraints (7)-(9) the penalty approach is employed as discussed in [40].

### 3.2. Hurricane occurrence model

The hurricane occurrence model is employed two times for each solution and each optimization algorithm iteration in the RDNEP structure. For the first time, after DNEP execution, the step of hurricane occurrence model is utilized to find the most vulnerable lines as the input of the resilient planning step to consider hardening efforts. Furthermore, the hurricane occurrence model is performed before the resilient operation scheduling for the second time in the proposed structure to provide an optimum situation based on the preventive and recovery network capability against the hurricane. Therefore, the outputs of steps #1 and #3 are considered as inputs of the hurricane occurrence model at the first and second times, respectively. Moreover, the outcomes of this step are considered as inputs of steps #3 and #4. Since the overhead lines are the most vulnerable to confront an excessive hurricane in an electric distribution network, the main aim of this step is the prediction of damaged lines in a hurricane situation. In the proposed hurricane occurrence model, hurricane speed and direction should be predicted and evaluated at first. Then, the failure probability of the

Eq. (12) is made from three terms. The first term of the suggested index computes the line deviation angle with the hurricane path. If the hurricane path is more perpendicular to a line, the line will be more vulnerable. Moreover, due to the elimination of the angle unit, the computed deviation should be divided into 90° as the maximum deviation angle to make possible the summation of different terms. Furthermore, due to considering the coordination of the hurricane speed with the line damage probability, the fragility curve of lines is implemented in the second term. How much the below area of the fragility curve is greater, the line will be more vulnerable. To make dimensionless the second term, the computed variables should be divided into the maximum value of the below area of the line fragility curve. Line importance is employed as the last term of Eq. (12). The quantity and priority of loads in the downstream area of each line evaluate its importance. Due to normalize the evaluated value, it should be divided into the maximum multiplication of loads quantity and priority. In this step, the lines that their VI index satisfies constraint (13) are considered as more probable damaged lines in the presence of a hurricane. It should be noted that  $B^D$  (i.e. vulnerability threshold) at the first time employment of this step (i.e. performed as pre-step of resilient planning ( $B_p^D$ )) should be higher than it at the second one (i.e. considered as pre-step of the resilient operation ( $B_o^D$ )) in each iteration of the NSGA-II algorithm as Eq. (14).

$$VI_j \geq B^D, B^D = \begin{cases} B_p^D & \text{inpre - step of the resilient planning} \\ B_o^D & \text{inpre - step of the resilient operation} \end{cases} \quad (13)$$

$$B_p^D \geq B_o^D \quad (14)$$

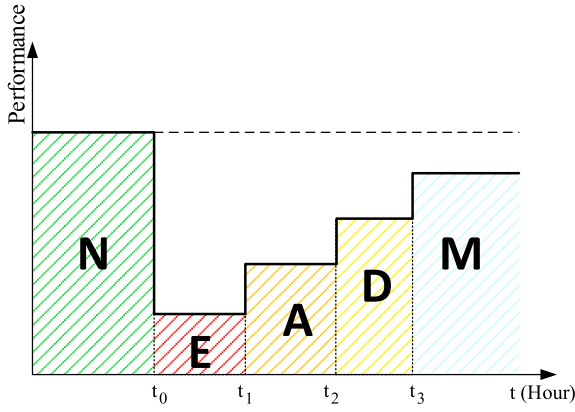


Fig. 4. Resilient operation states.

Therefore, the main computational burden of this step consists of evaluating load flow equations, determining the lines' difference angle, computing and sorting VI metrics for the whole lines of population members.

### 3.3. Resilient planning efforts

After determining the most vulnerable devices according to the hurricane occurrence model, resilient planning efforts are employed to reinforce the expanded distribution network capability against the HILP incidents. Here, line hardening measures, automatic switch allocation, and DGs sitting and sizing are considered as resilient planning efforts in order of their priorities. Therefore, this study proposes a three-step framework for resilient planning to increase the resilience potentials of a distribution system. In this way, the most vulnerable lines should be hardened as the first step. If the resilience budget is less than the hardening cost of the whole vulnerable lines, these lines should be prioritized based on Eq. (12) (i.e. VI index), and the most important and vulnerable lines will be hardened according to the resilience budget limitation as Eq. (15). In this section, the hardening cost (HC) is evaluated as Eq.(16):

$$\sum_{j \in \Omega^{V-L}} \sum_{t=1}^T \sum_{a=1}^{N_{type}^L} \frac{x_{j,t,a}^{L-H} \times L_j}{(1+r)^{t-1}} \times C^H < RB \quad (15)$$

$$HC = \sum_{j=1}^{N^L} \sum_{t=1}^T \sum_{a=1}^{N_{type}^L} \frac{x_{j,t,a}^{L-H} \times L_j}{(1+r)^{t-1}} \times C^H \quad (16)$$

The second step of the proposed resilient planning framework is implemented to allocate the automatic switches. In this step, all ti-lines should be equipped with automatic switches if limitation (17) is satisfied. Otherwise, the allocation of automatic switches will be performed by considering the ti-lines importance that is determined by Eq. (18) and the available planning budget. Furthermore, Eq. (19) evaluates the automation system cost (ASC).

$$\sum_{j=1}^{N^L} \sum_{t=1}^T \sum_{a=1}^{N_{type}^L} \frac{x_{j,t,a}^{T-L}}{(1+r)^{t-1}} \times IC_{Aus}^{Sw} \leq RB - HC \quad (17)$$

$$ASJ_j = \frac{\sum_{n \in \Omega_j^{p-L}} \gamma_n \times P_n^B}{\max(\sum_{n \in \Omega_1^{p-L}} \gamma_n \times P_n^B, \sum_{n \in \Omega_2^{p-L}} \gamma_n \times P_n^B, \dots, \sum_{n \in \Omega_{N^T-L}^{p-L}} \gamma_n \times P_n^B)}, \forall j \in \Omega^{T-L} \quad (18)$$

$$ASC = \sum_{j=1}^{N^T-L} \sum_{t=1}^T \sum_{a=1}^{N_{type}^{Sw}} \frac{x_{j,t,a}^{Sw}}{(1+r)^{t-1}} \times IC_a^{Sw} \quad (19)$$

Moreover, constraint (20) should be satisfied to implement DGs for reinforcing the network against HILP events as the third step. As this limitation, if the minimum investment cost of a DG type is less than the available resilience budget, this step will be performed. In this condition, Eq. (21) is applied to prioritize the buses that are not supported by other resilience resources for DGs allocation. According to the priority of buses, the available resiliency budget, and the damaged topology, optimum locations will be determined for DGs installation. Moreover, the size of DGs will be specified according to the remaining budget and vulnerable loads in the specified place. Furthermore, the investment cost of DGs is calculated as Eq. (22):

$$Min(DGC) \leq RB - HC - ASC \quad (20)$$

$$DGPI_n = \frac{\gamma_n \times P_n^B}{\max(\gamma_1 \times P_1^B, \gamma_2 \times P_2^B, \dots, \gamma_{N^{NHA}} \times P_{N^{NHA}}^B)} \forall n \in \Omega^{NHA} \quad (21)$$

$$DGC = \sum_{j=1}^{N^B} \sum_{t=1}^T \sum_{a=1}^{N_{type}^{DG}} \frac{x_{j,t,a}^{DG}}{(1+r)^{t-1}} \times IC_a^{DG} \quad (22)$$

Therefore, evaluating and sorting the allocation metrics of resilience resources such as DGPI, and ASI, as well as computation of their cost and considering the resiliency budget constraints, are the computational burden of this step to propose the optimum places for resilience resources. Furthermore, for the resilience budget constraint, if a less priority resilience resource causes the violation of this constraint, this resource will be omitted (i.e. its variable will be considered zero). Therefore, the resilience budget constraint will be satisfied.

### 3.4. Resilient operation strategy against hurricanes

After a hurricane occurrence, the proposed resilient operation strategy reduces the effects of the event, significantly. This study considers a five-state structure for the presented resilient operation scheduling as depicted in Fig. 2 and Fig. 4. Before starting the destructive effects of a hurricane, the network has a normal situation as the first state in the proposed structure (i.e. Normal state). The system robustness causes the network to preserve more this condition. In this situation, system variables are evaluated by power flow calculations. After destroying the network by a hurricane (i.e. Event state), the most vulnerable and not hardened lines are damaged. Therefore, a part of the loads will be isolated and not supplied. In this condition, power flow calculations based on the damaged network topology should be executed to determine the system specifications. Automatic switches as the most rapid resilience resources are implemented after a hurricane occurrence to reconfigure the network to minimize the not supplied loads as the third state (i.e. Automation state). Moreover, the power flow calculations are applied to determine the system variables in this situation. In the fourth state (i.e. DGs employment state), after spending DGs synchronization time, they will connect to the network and restore a part of lost loads. Power flow calculations in this step determine the network situation. Finally, manual switches are employed to isolate the damaged equipment and reconfigure the network to supply more lost loads as the operation fifth state (i.e. Manual switch employment state) of the proposed resilient operation strategy. The network will have been in this situation until the damaged elements will be repaired. As same as the previous steps, power flow equations are executed to evaluate the network variables. It can be concluded that the main computational burden of this step is the power flow calculations of each operation state.

### 3.5. Resilience evaluation

Due to evaluate different aspects of resiliency for a distribution network, this paper presents TFS indexes that are classified into technical, financial, and social welfare indexes (i.e. *TRI*, *ERI*, and *SWRI*, respectively). Moreover, the resilience index (*RI*) based on the above-mentioned aspects is proposed in this work as Eq. (23).

$$RI = TRI + ERI + SWRI \quad (23)$$

- Technical resilience indexes

The technical resilience index (*TRI*) as a per-unit value is based on the resilience operation curve according to Fig. 4 and the network supplied power. *TRI* consists of system robustness index (*SRI*), power adaptability index (*PAI*), and network recovery index (*NRI*) as follows:

$$TRI = \frac{SRI + PAI + NRI}{TRI^{Base}} \quad (24)$$

System robustness is the ability of a resilient distribution network that preserves the system from HILP incidents. This ability is related to the performed hardening efforts in the system that the proposed *SRI* index evaluates this capability of the network as Eq. (25).

$$SRI = \frac{\sum_{j=1}^{N^L} \sum_{a=1}^{N_{type}^{L-H}} x_{j,T,a}^{L-H} \times P_j^L}{\sum_{j=1}^{N^L} \sum_{a=1}^{N_{type}^{L-H}} x_{j,T,a}^L \times P_j^L} \quad (25)$$

*SRI* evaluates the supplied loads that are fed by the hardened lines as a per-unit value. In Eq. (25), If line *j* is hardened or underground, its  $x_{j,T,a}^{L-H}$  equals one and for other lines,  $x_{j,T,a}^{L-H}$  equals zero.

The system capability that prevents the effects of HILP events to go from damaged infrastructures to the not damaged parts of a distribution system is defined as the system adaptability that is a part of the resilience operation curve as shown in Fig. 4. Due to evaluate the system adaptability, this work suggests *PAI* as Eq. (26).

$$PAI = \frac{\sum_{j=1}^{N^B} P_j^{B,Min}}{\sum_{j=1}^{N^B} P_j^{B,R}} \quad (26)$$

*PAI* calculates the minimum supplied power of the network in the whole operation period of the hurricane condition as a per-unit number.

The system recovery is another resilience factor that shows the capability of a distribution network to restore the disconnected loads by automation devices, DGs, and manual switches as shown in Fig. 4. This study proposes *NRI* to evaluate the system recovery potential as Eq. (27).

$$NRI = \sum_{j=1}^{N^{T-L}} \sum_{a=1}^{N_{type}^{SW}} \sum_{n \in \Omega_j^{D-L}} \frac{x_{j,T,a}^{SW} \times P_n^B}{P_{TB} \times (T^R - t_{start})} \times (T^R - t_{start} - t_a^{SW}) + \sum_{j=1}^{N^B} \times \sum_{a=1}^{N_{type}^{DG}} \frac{x_{j,T,a}^{DG} \times P_a^{DG}}{P_{TB} \times (T^R - t_{start})} \times (T^R - t_{start} - t_a^{DG}) \quad (27)$$

*NRI* is constructed from two parts. Its first part evaluates the recovered energy of the isolated loads by different types of switches that are installed at the start node of ti-lines. It should be noted that all tie-lines are equipped with a type of switch (i.e. Automatic or manual). The second part of *NRI* calculates the recovered energy of the isolated loads by the DGs. As same as *SRI* and *PAI*, *NRI* is computed as a per-unit value to add with the other technical indexes.

- Economic resilience indexes

Economic resilience index (*ERI*) as Eq. (28) is based on the expansion planning cost ( $C_{Inv}$ ), resilience investment cost (*RIC*), damaged equipment cost (*DEC*), and load shedding cost (*LSC*) that are presented as follows:

$$ERI = \frac{ERI^{cons} - (C_{Inv} + RIC + DEC + LSC)}{ERI^{Base}} \quad (28)$$

In order to implement *ERI* for enhancing the system resiliency by maximizing its value as same as *TRI*,  $ERI^{cons}$  as a constant value is considered in Eq. (28) that is determined by sensitive analyzes. Moreover,  $ERI^{Base}$  is employed to evaluate *ERI* as a per-unit value. Moreover, *RIC* evaluates the investment cost of resilience resources such as DGs, automatic switches, and lines hardening actions according to Eq. (29):

$$RIC = HC + ASC + DGC \quad (29)$$

If a network is hardened, its vulnerability from a disaster decreases. Therefore, the replacement cost of damaged facilities such as overhead lines will be reduced when an HILP event occurred. In this study, *DEC* is formulated as Eq. (30) to evaluate the replacement cost of damaged lines as follows:

$$DEC = \sum_{j=1}^{N^L} \sum_{a=1}^{N_{type}^{D-L}} x_{j,T,a}^{D-L} \times L_j \times IC_a^L \times \dot{E}^{c,DEC} \quad (30)$$

Furthermore, *LSC* calculates load shedding cost during the event-affected operation duration as Eq. (31).

$$LSC = \int_{t_{start}}^{T^R} \sum_{j=1}^{N^B} P_j^{B,Shed} \times C^{Shed} \times d_t \quad (31)$$

- Social welfare resiliency index

In this study, the social welfare resiliency index (*SWRI*) as the number of supplied consumers during the hurricane-affected operation time is considered according to Eq. (32) as a per-unit number.

$$SWRI = \frac{\int_{t_{start}}^{T^R} \sum_{j=1}^{N^B} N_j^{D-C} \times d_t}{\int_{t_{start}}^{T^R} \sum_{j=1}^{N^B} N_j^C \times d_t} \quad (32)$$

### 3.6. NSGA-II optimization procedure

Due to the outputs of each step of RDNEP are used as inputs of the next steps, the proposed framework should be optimized by a sequential method. Moreover, the proposed RDNEP consists of two main objective functions. Hence, one of the multi-objective optimization approaches should be employed to optimize the problem. These approaches can take care of problems with unrelated objectives. These problems can be solved by two general methods[43]. In the priori approach as the first method, the combination of all objective functions is considered as a single objective to solve the problem by appropriate optimization methods. On the other hand, in the second strategy, namely posteriori method, nondominancy concept is applied to solve the multi-objective optimization problem. These approaches cause reach a set of pareto-optimal solutions, instead of a single solution. After that, the most appropriate solution can be selected based on the problem priorities. In this problem, the types of objectives are different. Hence, due to the applicability of the pareto-based approaches, these methods are employed here. The pareto-based approaches are classified as classical methods and heuristic techniques [44]. The multi-objective evolutionary algorithms (MOEAs) (i.e. heuristic techniques) can concurrently find a set of possible solutions which allow determining different members of the pareto- optimal set in a single run of the optimization algorithm. This feature can be considered as the main advantage of MOEAs. This is in opposition to the classical approaches, where a series of separate execution are essential. Moreover, MOEAs are not very sensitive to the continuity or shape of the pareto front and they can comfortably handle concave and discontinuous pareto fronts, while these subjects are a real challenge for classical approaches. Moreover,

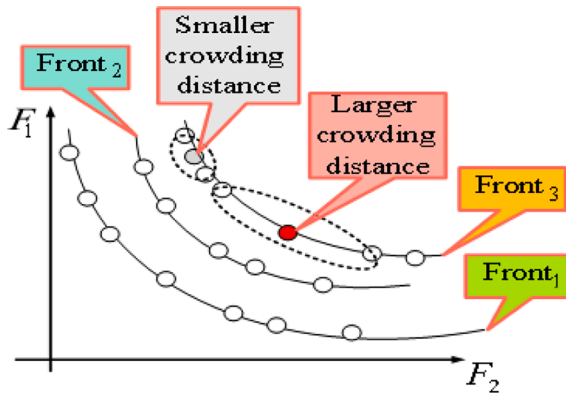


Fig. 5. Classification in NSGA-II algorithm.

they do not depend on specific information of the problem, they are simple to execute and they can be run in sequential processing environments [44]. According to [45], the NSGA-II is an elitist and fast multi-objective genetic algorithm. Moreover, this algorithm is an improvement and extension of NSGA with specialized multi-objective operators and mechanisms, i.e., crowding distance and non-dominated sorting. The NSGA-II has been generally implemented for multi-objective optimization problems, with high reliability and robustness. Moreover, common optimized algorithms such as the simulated annealing method, traditional genetic algorithm, and gradient approach are difficult to meet multi-objective optimization requirements. Based on [45], in most problems, NSGA-II can determine much better convergence close to the true pareto-optimal set and it is able to be evidenced exclusively prosperous in highly nonlinear problems. As discussed in [37] and [46], in comparison to other MOEAs, NSGA-II is efficient and has a proper convergence feature. Due to its diversity preserving characteristic, this method can maintain a proper spread of solutions. Moreover, there is no need to determine the sharing parameter and it has an easy yet efficient constraint-handling approach [43]. Therefore, the NSGA-II as one of the best accessible evolutionary algorithms is employed in this study. In order to optimize the above-mentioned problem, the outputs of DNEP and resilience evaluation steps in the main proposed framework are considered as the inputs of the NSGA-II optimization step as shown in Fig. 4. In this way,  $F_1$  and  $F_2$  based on the DNEP and resilience indexes are defined as NSGA-II objective functions according to Eqs. (33) and (34), respectively.

$$F_1 = F^{DNEP} \tag{33}$$

$$F_2 = \frac{1}{RI} \tag{34}$$

Based on the  $F_1$  and  $F_2$ , the solutions are classified as non-dominated sorting fronts according to Fig. 5 [47]. Then, the crowding distance will be evaluated for solutions of each non-dominated front as follows [38]:

$$cd_j = \sum_{i=1}^{N_f} \frac{F_i(j-1) - F_i(j+1)}{F_i^{max} - F_i^{min}}; j \in \Omega^s \tag{35}$$

where  $cd_j$  is the crowding distance for solution  $j$ . Then, the whole solutions should be checked that are classified [47]. After that, more optimum solutions will be considered as the new populations based on the high priority fronts and high crowding distance [47]. The crossover and mutation operators will be employed to optimize new solutions as the next step. In this situation, if the algorithm iterations are completed, the optimum constructed solutions will be comprised and the best solution will be proposed based on the TOPSIS approach [48]. Otherwise, the above-mentioned steps should be executed again. Hence, the calculations of NSGA-II and TOPSIS operators are the main computational burden of this step.

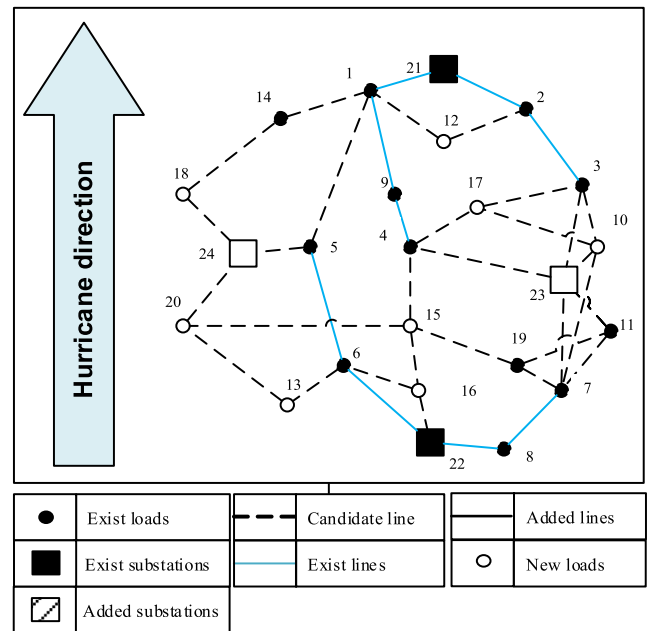


Fig. 6. The 24-node distribution network under study.

Table 3  
Load points data.

Bus	$P^B(t)(MW)$						$N^C$	$C^{shed} (\$/kWh)$	$\gamma$
	$t=0$	$t=1$	$t=2$	$t=3$	$t=4$	$t=5$			
1	2.54	2.59	2.63	2.70	2.73	2.74	17	38	5
2	0.50	0.60	0.62	0.63	0.67	0.71	25	24.5	1
3	1.66	1.75	1.93	1.88	1.96	2.04	20	24.1	3
4	0.29	0.30	0.32	0.24	0.29	0.29	40	27.8	4
5	1.05	1.17	1.22	1.28	1.33	1.45	20	24.5	4
6	0.75	0.90	0.92	0.92	0.98	1.2	23	29.9	4
7	2.87	2.16	2.37	2.38	2.84	2.85	33	24.5	5
8	0.46	0.47	0.51	0.56	0.56	0.59	20	24.5	3
9	0.80	0.88	0.93	0.95	0.96	1.03	3	30	4
10	0	1.19	1.30	1.43	1.63	1.65	21	24.5	3
11	0	1.17	1.25	1.34	1.44	1.67	9	17.5	1
12	0	0	0.62	0.65	0.69	0.79	19	17.5	2
13	0	0	0.78	0.81	0.83	0.88	24	17.5	2
14	0	0	0	2.14	2.15	2.15	12	24.8	3
15	0	0	0	1.13	1.13	1.13	10	20.1	3
16	0	0	0	1.51	1.54	1.60	14	29.9	4
17	0	0	0	0	0.66	0.74	16	20.1	3
18	0	0	0	0	0.96	1.03	34	32	5
19	0	0	0	0	0	1.09	26	29.9	5
20	0	0	0	0	0	2.65	22	24.5	4

It should be noted that the main novelty of this study is a framework for expanding a distribution network resiliently against the hurricane. The optimization method is not the main concentration and challenge of this study. However, NSGA-II is employed here that is a common and proper method in the power system problems (e.g. DNEP) based on the credible previous studies and references such as [38,47,49], and [50]. At last, it can be concluded that the proposed distribution network expansion planning model is constructed from technical, economic, and resilience-based objectives and constraints. In this way, investment cost (i.e. Eq. (1)), operation cost (i.e. Eq. (2)), and economic budget constraints (i.e. Eqs. (15), (17), and (20)) are considered as economic aspect of the proposed model. Moreover, the constraints of network radiality (i.e. Eqs. (4) and (5)), voltage (i.e. Eq. (9)), capacity (i.e. Eqs. (7) and (8)), and other power flow limitations are applied as the technical aspect of RDNEP. Furthermore, resilience indexes (i.e. Eqs. (23)-(32)) construct

**Table 4**

Data of conductors used in the existing network and for expansion.

Conductor	Type	Resistance $\Omega$ / km	Resistance $\Omega$ / km	Rated power (MVA)	Rated voltage (kV)
LA56	Overhead	0.683	0.415	3.4	20
XLPE	cable	0.202	0.204	8.1	20

the resilience feature of the proposed model. Therefore, the proposed RDNEP is a comprehensive framework that considers the resilience characteristics of the distribution network in addition to the economic and technical features.

**4. Numerical study**

In this section, the performance of the proposed RDNEP is discussed. It should be mentioned that all simulations are performed on a personal computer with Intel Core i5 CPU @3.20 GHz and 4 GB RAM in the Windows Professional 7 environment. RDNEP is formulated as an MINLP model and executed using the NSGA-II algorithm for developing the optimization algorithm in the multi-paradigm numerical computing environment and proprietary programming language matrix laboratory (i.e. MATLAB R2018b) and MATPOWER 4.1 M-files (function *runpf*) for power flow calculations [51]. Moreover, due to reach the more optimum solution as much as possible, RDNEP based on the NSGA-II is executed twenty times, independently. Then the best result of all repetitions is reported as the output of the proposed model. In this section, two case studies based on a 24-node distribution network and a real one are considered to evaluate the effectiveness of RDNEP as follows:

**4.1. Case A: A 24-node distribution network**

In this case, the proposed RDNEP is implemented on a 24-load point test grid depicted in Fig. 6. This grid is a 20-kV distribution network that is fed by two 20-MVA, 63-kV/20-kV substations. The suggested feasible paths and places for creating future substations and feeders are depicted in Fig. 6.

Table 3 illustrates the load points data, including the predicted peak power demand during five years. Furthermore, the priorities of loads based on their types (e.g. medical, military, industrial, commercial, and residential) are depicted in Table 3.

The line type that is employed in the existing grid is LA56 as an overhead line type. For system expansion, in addition to this conductor, the XLPE cable type can also be used. Table 4 provides the data related to

**Table 5**

Line data.

line	from	to	Length (km)	Deviation angle from the north (°)	line	from	to	Length (km)	Deviation angle from the north (°)
1	21	1	1	45	20	20	15	3.2	0
2	21	2	1.1	60	21	6	16	1.4	60
3	1	9	1.5	10	22	16	22	0.9	0
4	2	3	1.5	50	23	15	16	0.7	5
5	9	4	1.1	10	24	4	15	0.8	15
6	5	6	1.8	5	25	4	17	1.5	45
7	7	8	1.2	50	26	23	4	1.8	85
8	6	22	1.3	60	27	15	19	1.3	45
9	8	22	1.4	90	28	3	17	1.6	45
10	1	12	1.3	60	29	17	10	2.4	60
11	2	12	1.3	60	30	3	10	1.6	10
12	1	14	1.6	75	31	3	23	1.8	20
13	14	18	1.5	45	32	23	10	1.2	65
14	18	24	1.3	45	33	10	7	2.5	20
15	1	5	3.1	5	34	23	7	1.6	25
16	24	5	0.8	60	35	23	11	1.7	50
17	24	20	1.4	45	36	7	11	1.6	45
18	20	13	1.4	30	37	19	11	2.7	70
19	6	13	1.5	90	38	19	7	1.3	80

the line types.

Lines characteristics that consist of their start/end load point, length, and deviation angle from the north are presented in Table 5.

The parameters of the optimization algorithm are experimentally selected by sensitivity analysis as discussed in [52]. In this way, different parameter sets are employed based on typical values according to Table 6 [52] and [39]. After that, the parameters which cause the more optimum results are applied for the optimization algorithm. Therefore, the proper parameter set is determined as  $\rho_m = 0.01, \eta_c = 30, \rho_c = 0.9, \eta_c = 1, \eta_m = 10, \text{and } NS^{Opt} = 50$ .

The other required constants and parameters are considered in Table 7.

As presented in Fig. 6, the main hurricane path is presumed in the

**Table 6**

The NSGA-II parameter space.

Parameters	Values
$\rho_c$	0.3    0.5    0.7    0.9    1
$\eta_c$	10    30    50    100    200
$\rho_m$	0.001    0.005    0.01    0.05    0.1
$\eta_m$	10    30    50    100    200
$NS^{Opt}$	20    50    150    300    500

**Table 7**

Simulation parameters.

Parameters	Values	Parameters	Values
$IC_{30MVA}^{sb} (\$)$	900,000	$IC_{20MVA}^{sb} (\$)$	700,000
$IC_{LA56}^L (\$/km)$	8,500	$B_p^D$	1.5
$IC_{XLPE}^L (\$/km)$	20,000	$\dot{E}^{\circ} DEC$	5
$IC_{MS}^{Sw} (\$)$	10,000	$t^{DG} (\text{Hour})$	0.25
$IC_{AS}^{Sw} (\$)$	40,000	$B_0^D$	1
$OC^{sb} (\$/MVA)$	1000	$\sigma^{max} (m/s)$	55
$\delta_v$	0.05	$ERI^{Cons} (\$)$	2,900,000
$T^{Opt}$	1000	$ERI^{Base} (\$)$	1,500,000
$t_{start}$	07:00	$r$	0.1
$C^{Loss} (\$/kWh)$	0.06	$TRJ^{Base}$	2
$C^H (\$/km)$	8400	$T^R (\text{Hour})$	24
$IC_{1MW}^{DG} (\$)$	194,000	$t_{MS}^{SW} (\text{Hour})$	0.5
$IC_{0.5MW}^{DG} (\$)$	93,000	$t_{AS}^{SW} (\text{Hour})$	0.001
$RB (\$)$	282,000		

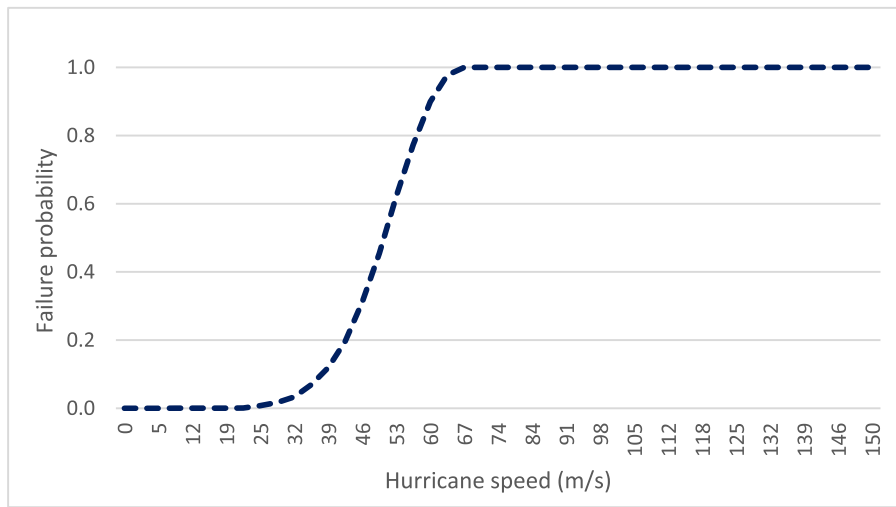
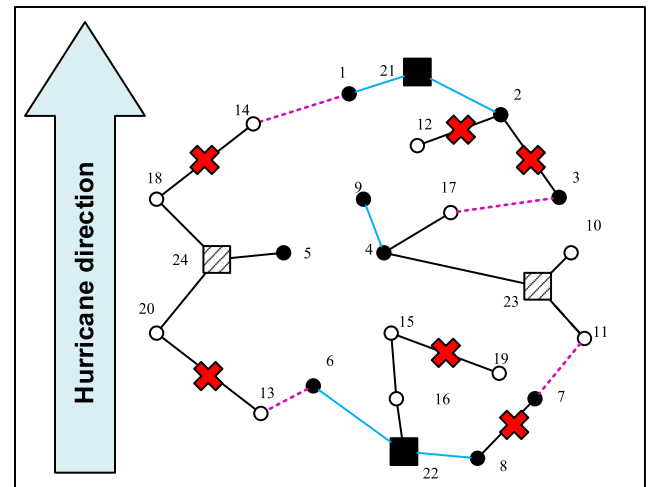


Fig. 7. An overhead distribution network line fragility curve against a hurricane.

Table 8  
Detail of dynamic RDNEP topology in scenario #1.

Element		Time duration				
		t = 1	t = 2	t = 3	t = 4	t = 5
Line	Removed	(1,2,8,9)	-	-	-	-
	Added	XLPE (1,2,8,9), LA56 (30,36)	LA56 (11,19)	XLPE (22), LA56 (12, 23)	LA56 (28,13)	LA56 (18,38)
Hardened lines		-	-	-	-	-
Tie-line	Consider	-	-	-	-	-
Substation	Added	-	-	-	-	-
DG	Added	-	-	-	-	-
Switch	Added	-	-	-	-	-



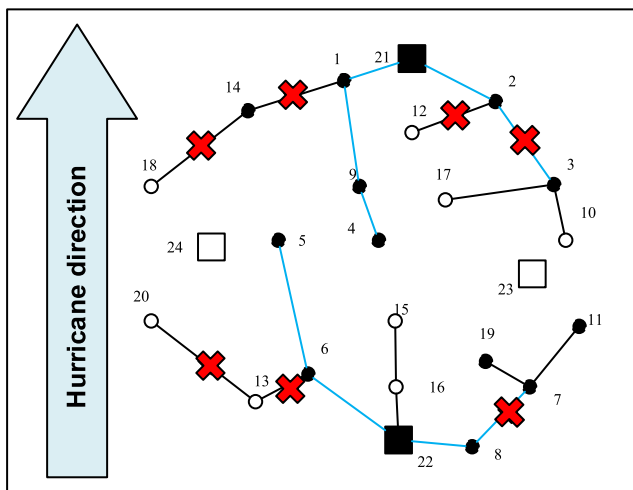
○	New loads	⋯	Tie-lines	▬	Added lines
●	Exist loads	—	Hardened lines	⊗	Damaged lines
■	Exist substations	- - -	Candidate line		
▨	Added substations	—	Exist lines		

Fig. 9. The proposed topology in scenario #2.

north and the above-mentioned system is considered as a one-zone and one-time interval against the hurricane. Moreover, Fig. 7 illustrates an overhead distribution system line fragility curve in the hurricane condition [24] that is employed to specify the most vulnerable lines based on the hurricane speed. It should be noted that the primary line of each feeder can be underground. The underground lines are not vulnerable in front of hurricanes.

In this case, three scenarios are studied on a 24-node distribution network to validate the performance of the presented model as follows:

**Scenario #1:** This scenario determines a distribution network expansion topology by a conventional strategy that is a cost-based model and optimized just by DNEP objective function. In this case, resilience resources and TFS metrics are not considered in the optimization procedure. However, the TFS metrics are evaluated for the proposed topology after DNEP execution to compare its resiliency capability with other scenarios. Table 8 presents the detail of the multistage plan that



○	New loads	⋯	Tie-lines	▬	Added lines
●	Exist loads	—	Hardened lines	⊗	Damaged lines
■	Exist substations	- - -	Candidate line		
▨	Added substations	—	Exist lines		

Fig. 8. The proposed topology in scenario #1.

**Table 9**  
Detail of dynamic RDNEP topology in scenario #2.

Element		Time duration				
		t = 1	t = 2	t = 3	t = 4	t = 5
Line	Removed	(1,2,8,9)	-	-	(3,6)	-
	Added (Line)	XLPE (35,32), LA56(36)	LA56 (11,19)	LA56 (23,12), XLPE (22)	LA56 (25,13,28) XLPE (14,16,26)	LA56 (18,27) XLPE (17)
Hardened lines		-	-	-	-	-
Tie-line	Consider	(36)	-	-	(12,28)	(19)
Substation	Added (node)	20 MVA (23)	-	-	20 MVA (24)	-
DG	Added (node)	-	-	-	-	-
Switch	Added (node)	Manual (11)	-	Manual (1)	Manual (3)	Manual (6)

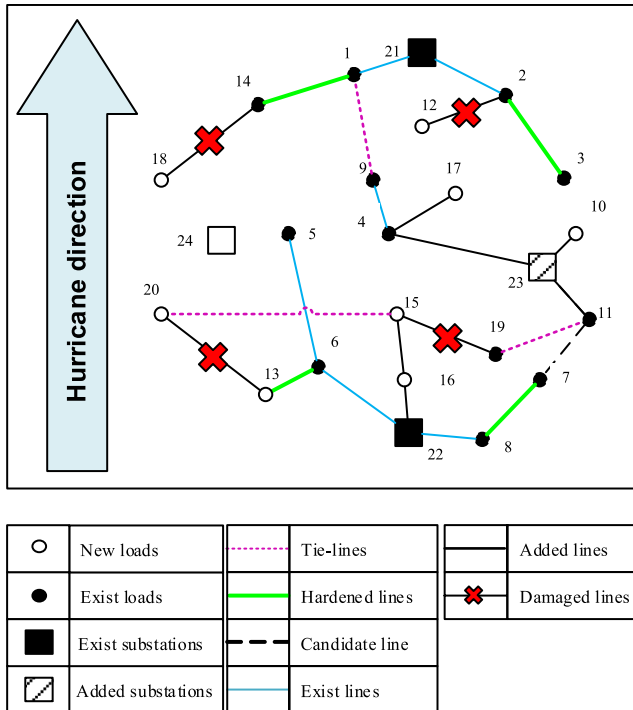


**Fig. 10.** The proposed topology in scenario #3.

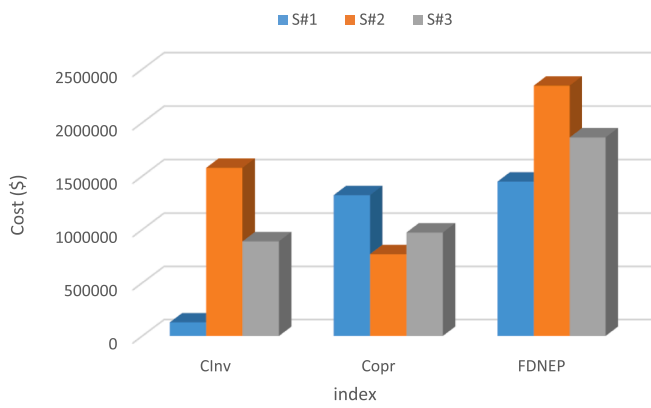
consists of the infrastructures that must be added/removed to/from the grid each year to expand the network based on the suggested plan. In this case, the lines (1–14), (2–3), (6–13), (14–18), (8–7), (2–12), and (13–20) are considered as the vulnerable lines that are anticipated as the destroyed lines in the hurricane condition by the suggested hurricane occurrence model as shown in Fig. 8. The proposed topology consists of

**Table 10**  
Detail of dynamic RDNEP topology in scenario #3.

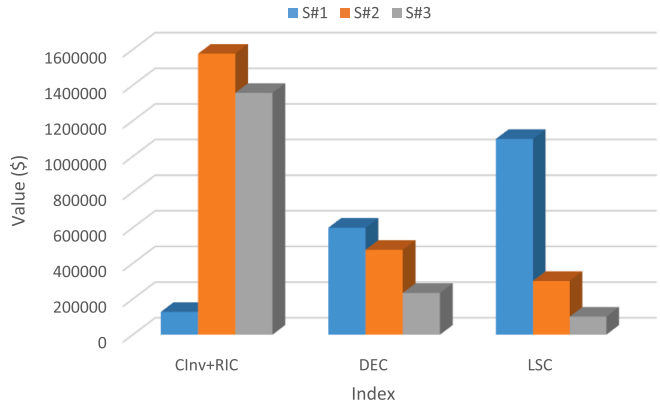
Element		Time duration				
		t = 1	t = 2	t = 3	t = 4	t = 5
Line	Removed	(1,2,8,9)	-	-	-	-
	Added	XLPE (1,2,8,9,35,32)	LA56 (11,19)	LA56 (12,23), XLPE (22)	LA56 (25,13) XLPE (26)	LA56 (18,38)
Hardened lines		(7,4)	(19)	(12)	(3)	(20,37)
Tie-line	Consider	-	-	-	(3)	(20,37)
Substation	Added (node)	20 MVA (23)	-	-	-	-
DG	Added (node)	-	-	-	(1 MVA) (18)	-
Switch	Added (node)	Automatic (1)	-	-	-	Automatic (11), (15)

the minimum number of substations (i.e. two substations) and the longest feeders in comparison with other ones according to Fig. 8. Therefore,  $F_{DNEP}$  and the investment cost of this scenario are the least in all cases as shown in Fig. 11.a. Furthermore, high length feeders of the proposed topology lead to an increase in the power losses and operation cost of this scenario more than other cases according to Fig. 11.a. Due to no presence of the TFS indexes in the optimization procedure and no presence of resilience resources, this scenario has the lowest *SRI*, *PAI*, and *NRI* indexes as shown in Fig. 11.b, as well as the *DEC* and *LSC* indexes of this plan that are in the worst situation as illustrated in Fig. 11. c. Therefore, the minimum *SWRI* and *TRI* belong to scenario #1 as depicted in Fig. 11.d. Moreover, the minimum *RIC* and investment cost lead to this case doesn't have the minimum *ERI*. It should be mentioned that the primary lines of feeders that are undergrounded, affect the TFS metrics in this scenario. Finally, due to the above-mentioned reasons, the proposed plan of scenario #1 has the lowest *RI* as shown in Fig. 11.e. It means that the suggested topology has the minimum resiliency against a hurricane in comparison with the proposed topology of other scenarios.

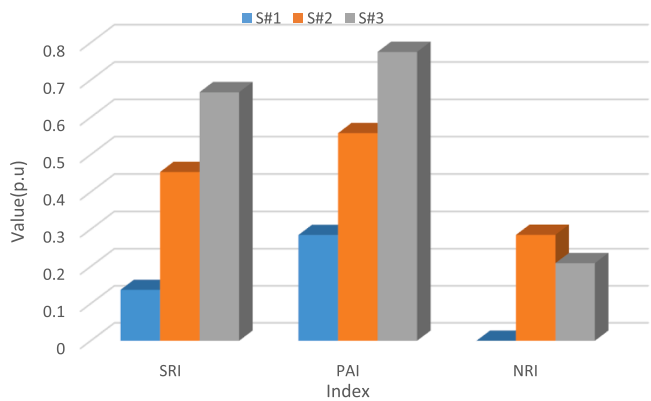
**Scenario #2:** In this scenario, the expanded topology is specified by the proposed resilience structure and without resilience resources. Fig. 9 and Table 9 present the proposed plan achieved in this case. According to this plan, two substations are added to the network in the first and fourth years of the planning horizon to increase the network resiliency and supply added loads. As depicted in Fig. 9, in this scenario, the proposed topology of the feeders is different from the scheme that is suggested by the cost-based model (i.e. scenario #1). More clarification about the proposed dynamic RDNEP plan of scenario #2 is presented in Fig. 9. Based on the suggested hurricane occurrence structure as illustrated in Fig. 9, the lines (1–14), (13–20), (2–3), and (7–8) are considered as the vulnerable lines that are predicted as the damaged lines in the hurricane condition. As shown in Fig. 11.a, due to the employment of two new substations, this scenario has the most investment cost in comparison with other ones. Moreover, the decrement of feeders length and increment of substations number lead to be the



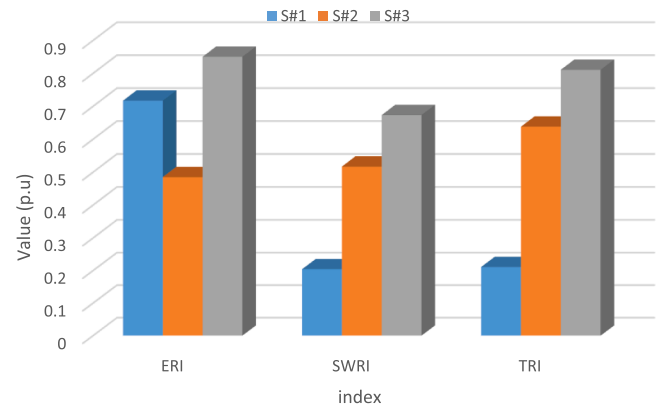
(a) Comparison of DNEP objective function and costs



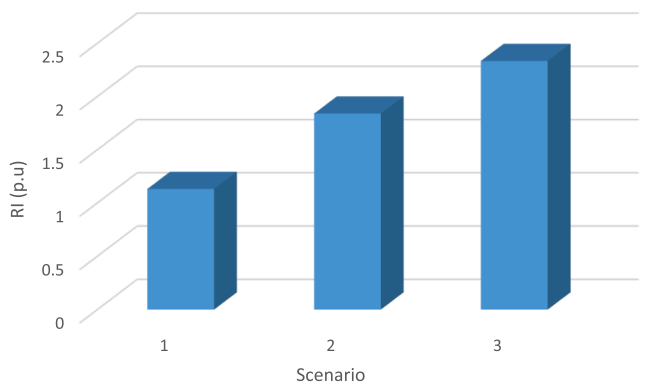
(c) Comparison of economic indexes for resiliency in scenario #1-#3



(b) Comparison of technical indexes



(d) Comparison of ERI, TRI, and SWRI indexes



(e) Comparison of RI

Fig. 11. Comparison of DNEP objective function and TFS indexes in scenario #1-#3.

operation cost of this scenario is significantly less than scenario #1 according to Fig. 11.a. On the other hand, the very high investment cost of substations causes the maximum value of  $F_{DNEP}$  is calculated in this scenario as shown in Fig. 11.a. Moreover, the proposed resilience structure employment in this scenario leads to achieving a topology that the whole proposed technical indexes (i.e. SRI, PAI, NRI, and TRI), as well as some financial indexes (i.e. DEC and LSC), are promoted in comparison with scenario #1 as depicted in Fig. 11.b and Fig. 11.c, respectively. It should be noted that the SRI index is directly related to the number of primary lines of feeders that are undergrounded and not vulnerable against the hurricane. Due to the very high investment cost of this topology and no significant improvement of DEC and LSC indexes,

this scenario has the minimum ERI as shown in Fig. 11.d. Moreover, the proposed topology of this case leads to TRI and SWRI metrics be more than these indexes in scenario #1. Eventually, as illustrated in Fig. 11.e, according to the above-mentioned analysis and reasons, the resiliency capability of the proposed topology in scenario #2 is higher than scenario #1 and less than scenario #3 based on the RI index.

**Scenario #3:** In this case, DNEP is performed by the proposed resilience and cost-based structure in presence of resilience resources. The achieved topology of this scenario is depicted in Fig. 10. More detail of the proposed dynamic plan for this scenario is presented in Table 10. In the proposed topology, lines (1-14), (6-13), (8-7), and (2-3) as well as all tie-lines are suggested to be hardened. Based on the proposed

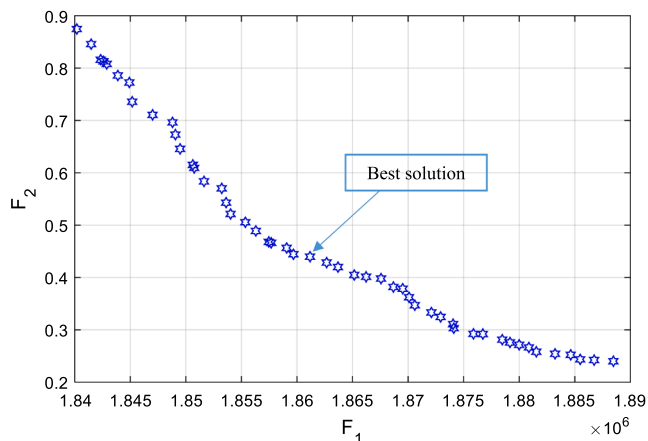


Fig. 12. A Pareto surface for optimal RDNEP identified by the suggested framework.

Table 11  
RDNEP sensitivity analyzes data in scenario #3.

Resiliency budget level	RB (\$)	Vulnerability threshold level	$B_p^D$
1	46,000	1	1.9
2	70,000	2	1.7
3	282,000	3	1.5
4	476,000	4	1.3

hurricane model and VI index, the lines (2–12), (13–20), (15–19), and (14–18) are recognized as the vulnerable lines that are probability damaged in the hurricane situation. Due to the employment of the cost-based and resilience-based indexes in DNEP as well as resilience resources, simultaneously, scenario #3 has the most optimum situation in both resiliency and cost aspects, concurrently, in comparison with other scenarios. Employment of both expansion and resilience infrastructures leads to the reduction of the investment cost and  $F_{DNEP}$  in this case in comparison with scenario #2 as shown in Fig. 11.a. Moreover, Fig. 11.a shows that the operation cost of this case is close to scenario#2 and less than the operation cost of case #1. Employment of hardening strategies, automatic switches, tie-lines, and DGs leads to promote network robustness and adaptability more than other cases as shown in Fig. 11.b. Moreover, the recovery capability of this case is close to scenario#2 and better than scenario #1 according to the NRI value that is presented in Fig. 11.b. Furthermore, in this case, resilience efforts decrease the LSC and DEC more than in other cases and the summation of RIC and  $C_{Inv}$  is less than scenario#2 according to Fig. 11.c. Due to employing resilience resources and the proposed resilience-based framework, the maximum values of ERI, SWRI, and TRI indexes happen in this case as depicted in Fig. 11.d. At last, distribution network expansion and reinforcement topology, resilience resources planning, and resilient scheduling improve the resiliency of the network against a hurricane occurrence based on the RI index that is illustrated in Fig. 11.e in comparison with other scenarios.

In this case, Fig. 12 illustrates the set of non-dominated solutions and the best compromise solution with the equal priority of the objective functions.

To evaluate the effects of different RBs and several predefined vulnerability threshold levels on the RDNEP study, multifarious cases are defined according to Table 11 in scenario #3 to execute a sensitivity analysis as shown in Fig. 13.

Fig. 13 shows the manner of TRI, SWRI, ERI, and RI metrics based on different resiliency budget levels (i.e. RB) and vulnerability threshold levels (i.e.  $B_p^D$ ). Reduction of  $B_p^D$  generally leads to TRI, RI, SWRI, and ERI decrement. The maximum reduction of mentioned metrics occurs in the second vulnerability level and its minimum happens in the fourth one.

As shown in Fig. 13, if the  $B_p^D$  is less than 1.5, the network vulnerability is close to the condition that its  $B_p^D$  is 1.5. Therefore, investigation of the situations that their  $B_p^D$  levels are less than 1.5 can be ignored in the RDNEP study. On the other hand, the RB increment generally improves TRI and SWRI. The second RB level leads to the maximum improvement of the TRI, SWRI, ERI, and RI metrics. However, in the fourth RB level, TRI and SWRI don't experience significant enhancement. Moreover, in this condition, the ERI and RI metrics are reduced as depicted in Fig. 13.c and Fig. 13.d, respectively, due to the high investment cost of the employed resilience resources and no significant improvement of TRI and SWRI. Therefore, the RDNEP study is not necessary by the budgets that are more than the third RB level.

In order to validate the proposed model, RDNEP is also solved by the multi-objective particle swarm optimization (MOPSO) algorithm [53] and the multi-objective evolutionary algorithm based on decomposition (MOEA/D) [54] using MATLAB to evaluate the efficacy and feasibility of the proposed optimization method. As discussed in reference [55], inverted generational distance (IGD), spacing (SP), and maximum spread (MS) metrics are implemented to compare the capability of the multi-objective algorithms. IGD is used to evaluate the convergence, spacing (SP), and maximum spread (MS) metrics are implemented to measure the coverage of the multi-objective algorithms [55]. The competence of the suggested algorithm is depicted by the comparison of NSGA-II, MOEA/D, and MOPSO. In this way, the above-mentioned algorithms are implemented in the third scenario of case#1 that the whole proposed framework is employed. Table 12 illustrates the capability comparison of the suggested approach. This table presents the IGD comparison of the above-mentioned algorithms and it is depicted that NSGA-II gives better results as compare to MOEA/D and MOPSO for this problem. Moreover, Table 12 illustrates the index of spacing comparison and it is shown that standard deviation (Std. dev.), average, worst, and best values of NSGA-II are more stable than the MOEA/D and MOPSO. It shows that non dominated pareto solution of NSGA-II is more distributed. It is also illustrated in Table 12 that the index of spread for NSGA-II is again better than the MOEA/D and MOPSO. This MS concludes that the distance between the space covered by the solutions and boundary solutions is better in NSGA-II.

Moreover, the comparison of RDNEP objective functions (i.e.  $F_{DNEP}$  and RI) that are optimized by the above-mentioned multi-objective optimization methods and the same multiple criteria decision-making method (i.e. TOPSIS) is presented in Table 13. It shows that the NSGA-II method can find more optimum solutions than other ones.

Furthermore, Table 14 depicts the comparison of economic-based [56], reliability-driven [39], and resilience-based (i.e. RDNEP as the proposed model) frameworks for distribution network expansion planning. It shows that the RDNEP expands a distribution network more resiliently than other frameworks with an optimum cost. Moreover, the economic-based model has the minimum DNEP cost (i.e.  $F_{DNEP}$ ). However, its resilience capability is the worst in comparison with other strategies. The reliability-driven model provides expansion planning with DNEP cost close to resilience-based one but its resiliency performance is significantly lower than RDNEP and better than economic-based strategy.

#### 4.2. Case B: A real distribution network

In order to evaluate the proposed RDNEP model on a real distribution network, two feeders are considered that are placed in the Ghale-Ganj district of Kerman, Iran. These feeders are named Tarikmah and Ahovan. Fig. 14 depicts the topology of the above-mentioned grid based on Geographische Information System (GIS) data. This grid consists of 402 available buses, one 63/20 kV substation, 27 new buses, 52 candidate lines, and 349 available lines. The required constants and parameters for the simulation of this case are considered according to case A. In order to evaluate the effect of the proposed RDNEP on the

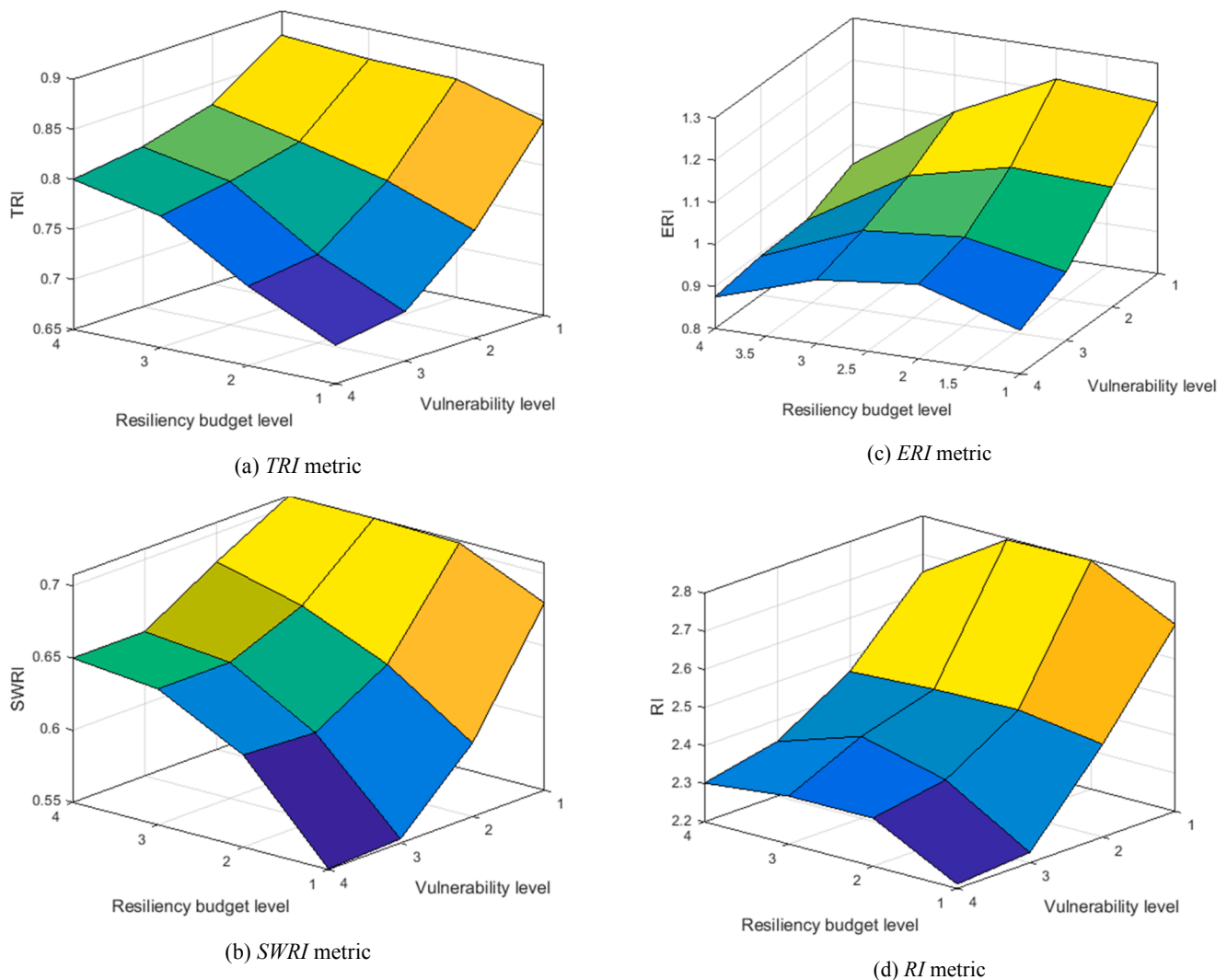


Fig. 13. Sensitivity analysis based on TFS metrics.

Table 12  
Comparison of IGD, SP, and MS metrics.

Index	IGD			SP			MS		
	NSGA-II	MOPSO	MOEA/D	NSGA-II	MOPSO	MOEA/D	NSGA-II	MOPSO	MOEA/D
Avg.	0.0028	0.0182	0.0658	0.0714	0.1317	0.2108	1.1007	1.0521	0.9654
Std.dev.	0.0007	0.0041	0.0361	0.0291	0.0724	0.1158	0.1139	0.2262	0.3021
Worst	0.0059	0.0353	0.1073	0.1742	0.4131	0.6645	1.9761	1.8561	1.7313
Best	0.0018	0.0105	0.0206	0.0403	0.0411	0.0661	1.2914	1.2124	1.1567

Table 13  
Comparison of different optimization methods.

Index	NSGA-II	MOPSO	MOEA/D
$F_{DNEP}(\$)$	1,356,270	1,373,164	1,389,656
RI	2.334	2.193	2.015

Table 14  
Comparison of different DNEP strategies.

Index	Economic-based	Reliability-driven	RDNEP
$F_{DNEP}(\$)$	127,500	1,410,446	1,411,576
RI	1.132	1.754	2.334

mentioned real distribution network, two scenarios (i.e. DNEP and RDNEP) are studied on the above-mentioned network. The results of these scenarios are presented in Table 15. Employment of cost-based objectives leads to the reduction of the investment cost and  $F_{DNEP}$  of DNEP in comparison with RDNEP in the real case as shown in Table 15. Moreover, due to the DG implementation and the proposed topology in the RDNEP scenario, the power losses and the operation cost of this scenario are lower than the DNEP scenario. Furthermore, employment of resilience resources and the combination of resilience-based and cost-based objectives promote network resiliency and capability of RDNEP scenario more than DNEP scenario as shown in Table 15.

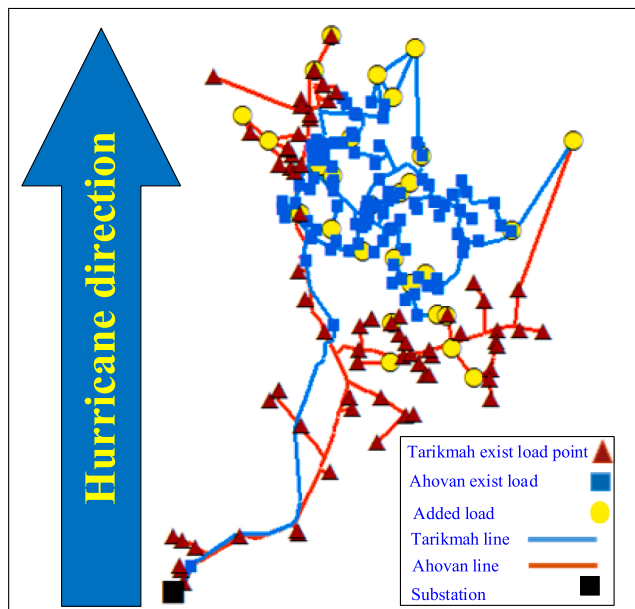


Fig 14. The Ghale-Ganj 20 kV distribution network.

Table 15  
Results of the real case evaluation.

Indexes	DNEP	RDNEP (Proposed model)
$C_{Inv}$ (\$)	510,000	3,357,600
$C_{Opt}$ (\$)	1,717,084	1,263,108
$F_{DNEP}$ (\$)	2,227,084	4,620,708
$SRI$	0.061	0.298
$PAI$	0.078	0.211
$NRI$	0.000	0.129
$TRI$	0.069	0.319
$ERI$	0.742	0.776
$RIC$ (\$)	0.000	3062850.000
$DEC$ (\$)	3932578.125	1533984.375
$LSC$ (\$)	4047706.864	127954.077
$SWRI$	0.031	0.101
$RI$	0.842	1.737

## 5. Conclusion

This paper proposes a multistage, dynamic, and resilient-based structure for distribution network expansion and reinforcement planning that is named resilient distribution network expansion planning (RDNEP) to supply existing and new loads confidently against hurricanes. The suggested framework considers distribution network expansion planning (DNEP), hurricane concurrence model, resilient resources planning, resilient operation, the technical, financial, and social welfare resiliency indexes for resiliency evaluation, and a multi-objective optimization method that constructs six steps of the RDNEP. In the first step of the presented structure, investment and operation costs are applied as the expansion planning objective functions to specify expansion topology. Then, a hurricane occurrence model is employed to determine the most vulnerable lines. In the third step, resilience resources planning is performed to reinforce the network based on the outputs of previous steps. After that, the hurricane occurrence model is employed again to apply resilient operation strategies based on the network preventive capabilities to have the best performance against the hurricane. Then, the resiliency evaluation section is performed based on technical, financial, and social welfare resiliency indexes to assess the performance of the proposed framework. Moreover, the non-dominated sorting

genetic algorithm II optimization method combined with the technique for order preference by similarity to ideal solution approach is employed to determine the optimum solution. In order to execute and evaluate the proposed model, two cases are considered based on a 24-node distribution network and a real one. In the 24-bus distribution network, three scenarios are defined as conventional DNEP, RDNEP without resilience resources, and combined conventional and RDNEP in presence of resilience resources as the proposed model. The numerical results show that the conventional DNEP, due to considering the cost-based objective functions, has the minimum resilience level. Moreover, the RDNEP outcome is more resilient than scenario #1. However, its DNEP objective function is very higher than the other scenarios. The proposed framework execution as the third scenario shows that the suggested RDNEP has a more optimum situation in DNEP objective function and resiliency indexes in comparison with other models and scenarios. Furthermore, the execution of the RDNEP in the real case shows the effectiveness of the proposed model on the resiliency capability of distribution networks. Finally, the authors suggest employing energy storage planning and scheduling as further works in the proposed structure.

## CRedit authorship contribution statement

**Amirhossein Nasri:** Conceptualization, Methodology, Software. **Amir Abdollahi:** Supervision, Visualization, Investigation, Validation, Writing – review & editing. **Masoud Rashidinejad:** Visualization, Investigation, Validation.

## Declaration of Competing Interest

The authors declare that they have no known competing financial interests or personal relationships that could have appeared to influence the work reported in this paper.

## References

- [1] Vahidinasab V, Tabarzadi M, Arasteh H, Alizadeh MI, Mohammad Beigi M, Sheikhzadeh HR, et al. "Overview of Electric Energy Distribution Networks Expansion Planning", *IEEE*. Access 2020;8:34750–69.
- [2] Heidari S, Fotuhi-Firuzabad M, Lehtonen M. Planning to Equip the Power Distribution Networks with Automation System. *IEEE Trans Power Syst* 2017;32(5):3451–60.
- [3] Xing H, Cheng H, Zhang Y, Zeng P. Active distribution network expansion planning integrating dispersed energy storage systems. *IET Gener Transm Distrib* 2016;10(3):638–44.
- [4] Gouin V, Alvarez Herault M-C, Raison B. Stochastic integration of demand response and reconfiguration in distribution network expansion planning. *IET Gener Transm Distrib* 2018;12(20):4536–45.
- [5] Nasri A, Abdollahi A, Rashidinejad M, Hadi Amini M. Probabilistic-possibilistic model for a parking lot in the smart distribution network expansion planning. *IET Gener Transm Distrib* 2018;12(13):3363–74.
- [6] Muñoz-Delgado G, Contreras J, Arroyo JM. Distribution System Expansion Planning Considering Non-Utility-Owned DG and an Independent Distribution System Operator. *IEEE Trans Power Syst* 2019;34(4):2588–97.
- [7] Lavorato M, Rider MJ, Garcia AV, Romero R. A constructive heuristic algorithm for distribution system planning. *IEEE Trans Power Syst* 2010;25(3):1734–42.
- [8] Cossi AM, da Silva LGW, Lázaro RAR, Mantovani JRS. Primary power distribution systems planning taking into account reliability, operation and expansion costs. *IET Gener Transm Distrib* 2012;6(3):274.
- [9] Naderi E, Seifi H, Sepasian MS. A dynamic approach for distribution system planning considering distributed generation. *IEEE Trans Power Deliv* 2012;27(3):1313–22.
- [10] Panteli M, Mancarella P. Influence of extreme weather and climate change on the resilience of power systems: Impacts and possible mitigation strategies. *Electr Power Syst Res* 2015;127:259–70.
- [11] Panteli M, Trakas DN, Mancarella P, Hatziaargyriou ND. Power Systems Resilience Assessment: Hardening and Smart Operational Enhancement Strategies. *Proc IEEE* 2017;105(7):1202–13.
- [12] Hu B, Li M, Niu T, Zhou P, Li Y, Xie K, et al. Hardening planning of overhead distribution lines in typhoon-prone areas by considering the typhoon motion paths and the line load reliability. *Int J Electr Power Energy Syst* 2021;129.
- [13] Wang X, Li Z, Shahidehpour M, Jiang C. Robust Line Hardening Strategies for Improving the Resilience of Distribution Systems with Variable Renewable Resources. *IEEE Trans Sustain Energy* 2019;10(1):386–95.
- [14] Tan Y, Das AK, Arabshahi P, Kirschen DS. Distribution systems hardening against natural disasters. *IEEE Trans Power Syst* 2018;33(6):6849–60.

- [15] Peng L, Hu B, Xie K, Tai HM, Yan J, Zhou J. Analytical model of power system hardening planning for long-term risk reduction. *Int J Electr Power Energy Syst* 2021;125.
- [16] C. He, C. Dai, L. Wu, and T. Qi, "Robust Network Hardening Strategy for Enhancing Resilience of Integrated Electricity and Natural Gas Distribution Systems Against Natural Disasters," pp. 1–1, 2020.
- [17] Bagheri A, Zhao C, Qiu F, Wang J. Resilient Transmission Hardening Planning in a High Renewable Penetration Era. *IEEE Trans Power Syst* 2019;34(2):873–82.
- [18] A. Najafi Tari, M. S. Sepasian, and M. Tourandaz Kenari, "Resilience assessment and improvement of distribution networks against extreme weather events," *Int. J. Electr. Power Energy Syst.*, vol. 125, 2021.
- [19] Yao F, Chau TK, Zhang X, Iu HHC, Fernando T. An Integrated Transmission Expansion and Sectionalizing-Based Black Start Allocation of BESS Planning Strategy for Enhanced Power Grid Resilience. *IEEE Access* 2020;8:148968–79.
- [20] Wang H, Jin T. Prevention and Survivability for Power Distribution Resilience: A Multi-Criteria Renewables Expansion Model. *IEEE Access* 2020;8:88422–33.
- [21] Najafi J, Peiravi A, Guerrero JM. Power distribution system improvement planning under hurricanes based on a new resilience index. *Sustain Cities Soc* 2018;39:592–604.
- [22] Borghesi M, Ghassemi M. Optimal planning of microgrids for resilient distribution networks. *Int J Electr Power Energy Syst* 2021;128.
- [23] Poudel S, Dubey A, Bose A. Risk-Based Probabilistic Quantification of Power Distribution System Operational Resilience. *IEEE Syst J* 2019;1–12.
- [24] Panteli M, Trakas DN, Mancarella P, Hatzigiargyriou ND. Boosting the Power Grid Resilience to Extreme Weather Events Using Defensive Islanding. *IEEE Trans Smart Grid* 2016;7(6):2913–22.
- [25] Sanjari I, Abdollahi A, Rashidinejad M, Afzali P, Arasteh H. A new fuzzy model for investigating the effects of lightning on the risk-based self-scheduling strategy in a smart grid. *Int J Electr Power Energy Syst* 2021;129.
- [26] Confrey J, Etemadi AH, Stuban SMF, Eveleigh TJ. Energy Storage Systems Architecture Optimization for Grid Resilience with High Penetration of Distributed Photovoltaic Generation. *IEEE Syst J* 2020;14(1):1135–46.
- [27] Chong W, Yunhe H, Feng Q, Shunbo L, Kai L. Resilience Enhancement With Sequentially Proactive Operation Strategies. *IEEE Trans Power Syst* 2017;32(4):2847–57.
- [28] Sang Y, Xue J, Sahraei-Ardakani M, Ou G. An Integrated Preventive Operation Framework for Power Systems During Hurricanes. *IEEE Syst J* 2019;1–11.
- [29] Huang G, Wang J, Chen C, Qi J, Guo C. Integration of Preventive and Emergency Responses for Power Grid Resilience Enhancement. *IEEE Trans Power Syst* 2017;32(6):4451–63.
- [30] Nguyen T, Wang S, Alhazmi M, Nazemi M, Estebars A, Dehghanian P. Electric Power Grid Resilience to Cyber Adversaries: State of the Art. *IEEE Access* 2020;8:87592–608.
- [31] G. Liu, T. B. Ollis, Y. Zhang, T. Jiang, and K. Tomsovic, "Robust Microgrid Scheduling With Resiliency Considerations," *IEEE Access*, pp. 1–1, 2020.
- [32] Gholami A, Shekari T, Aminifar F, Shahidehpour M. Microgrid Scheduling with Uncertainty: The Quest for Resilience. *IEEE Trans Smart Grid* 2016;7(6):2849–58.
- [33] Khodaei A. Resiliency-oriented microgrid optimal scheduling. *IEEE Trans Smart Grid* 2014;5(4):1584–91.
- [34] Wang Y, Rousis AO, Strbac G. Resilience-Driven Modeling, Operation and Assessment for a Hybrid AC/DC Microgrid. *IEEE Access* 2020;8:139756–70.
- [35] Amiroun MH, Aminifar F, Lesani H, Shahidehpour M. Metrics and quantitative framework for assessing microgrid resilience against windstorms. *Int J Electr Power Energy Syst* 2019;104:716–23.
- [36] Panwar M, Chanda S, Mohanpurkar M, Luo Y, Dias F, Hovsapian R, et al. Integration of flow battery for resilience enhancement of advanced distribution grids. *Int J Electr Power Energy Syst* 2019;109:314–24.
- [37] Deb K, Pratap A, Agarwal S, Meyarivan T. A fast and elitist multiobjective genetic algorithm: NSGA-II. *IEEE Trans Evol Comput* Apr. 2002;6(2):182–97.
- [38] Nejadfard-Jahromi S, Rashidinejad M, Abdollahi A. Multistage distribution network expansion planning under smart grids environment. *Int J Electr Power Energy Syst* 2015;71:222–30.
- [39] Heidari S, Fotuhi-Firuzabad M, Kazemi S. Power Distribution Network Expansion Planning Considering Distribution Automation. *IEEE Trans Power Syst* May 2015;30(3):1261–9.
- [40] Yen GG. An adaptive penalty function for handling constraint in multi-objective evolutionary optimization. *Stud Comput Intell* 2009;198:121–43.
- [41] Nasri A, Abdollahi A, Rashidinejad M. Probabilistic-proactive distribution network scheduling against a hurricane as a high impact-low probability event considering chaos theory. *IET Gener Transm Distrib* 2021;15(2):194–213.
- [42] Amiroun MH, Aminifar F, Lesani H. Resilience-Oriented Proactive Management of Microgrids Against Windstorms. *IEEE Trans Power Syst* 2018;33(4):4275–84.
- [43] Lee KY, El-Sharkawi MA. Evolutionary multiobjective optimization. *Mod Heuristic Optim Tech Theory Appl to Power Syst* 2007:1–586.
- [44] E. Zitzler, "Evolutionary Multiobjective Optimization," in *Handbook of Natural Computing*, G. Rozenberg, T. Bäck, and J. N. Kok, Eds. Berlin, Heidelberg: Springer Berlin Heidelberg, 2012, pp. 871–904.
- [45] Gao S, Bo C, Li J, Niu C, Lu X. Multi-objective optimization and dynamic control of biogas pressurized water scrubbing process. *Renew Energy* 2020;147:2335–44.
- [46] Tan TH. *Kay Chen, Khor, Eik Fun, Lee. Multiobjective Evolutionary Algorithms and Applications*: Springer; 2005.
- [47] Hu Y, Bie Z, Ding T, Lin Y. An NSGA-II based multi-objective optimization for combined gas and electricity network expansion planning. *Appl Energy* 2016;167:280–93.
- [48] Goh HH, Kok BC, Yeo HT, Lee SW, Mohd AA. Zin, "Combination of TOPSIS and AHP in load shedding scheme for large pulp mill electrical system". *Int J Electr Power Energy Syst* 2013;47(1):198–204.
- [49] Farzin H, Fotuhi-Firuzabad M, Moeini-Aghtaie M. A Stochastic Multi-Objective Framework for Optimal Scheduling of Energy Storage Systems in Microgrids. *IEEE Trans Smart Grid* 2017;8(1):117–27.
- [50] Soroudi A, Ehsan M. A distribution network expansion planning model considering distributed generation options and techno-economical issues. *Energy Aug.* 2010;35(8):3364–74.
- [51] Zimmerman RD, Murillo-Sánchez CE, Thomas RJ. MATPOWER: Steady-state operations, planning, and analysis tools for power systems research and education. *IEEE Trans Power Syst* 2011;26(1):12–9.
- [52] Wang R, Mansor MM, Purshouse RC, Fleming PJ. An analysis of parameter sensitivities of preference-inspired co-evolutionary algorithms. *Int J Syst Sci* 2015;46(13):2407–20.
- [53] C. A. C. Coello, G. T. Pulido, and M. S. Lechuga, "Handling multiple objectives with particle swarm optimization," *IEEE Trans. Evol. Comput.*, vol. 8, p. 256–279, 2004.
- [54] Zhang Q, Li H. MOEA/D: A multiobjective evolutionary algorithm based on decomposition. *IEEE Trans Evol Comput* 2007;11(6):712–31.
- [55] Mirjalili S, Saremi S, Mirjalili SM, Coelho LDS. Multi-objective grey wolf optimizer: A novel algorithm for multi-criterion optimization. *Expert Syst Appl* 2016;47:106–19.
- [56] Amjadi N, Attarha A, Dehghan S, Conejo AJ. Adaptive Robust Expansion Planning for a Distribution Network with DERS. *IEEE Trans Power Syst* 2018;33(2):1698–715.